Reconstructing the flow pattern evolution in inner region of the Fennoscandian Ice Sheet by glacial landforms from Gausdal Vestfjell area, south-central Norway

Artūrs Putniņš [a], *, Mona Henriksen [a]

[a] Faculty of Environmental Sciences and Natural Resource Management, Norwegian University of Life Sciences, P.O. Box 5003, 1432 Ås, Norway

* Corresponding author. Tel. +47 67231815. E-mail address: arturs.putnins@nmbu.no

Abstract

More than 17 000 landforms from detailed LiDAR data sets have been mapped in the Gausdal Vestfjell area, south-central Norway. The spatial distribution and relationships between the identified subglacial bedforms, mainly streamlined landforms and ribbed moraine ridges, have provided new insight on the glacial dynamics and the sequence of glacial events during the last glaciation. This established evolution of the Late Weichselian ice flow pattern at this inner region of the Fennoscandian Ice Sheet is stepwise where a topography independent ice flow (Phase I) are followed by a regional (Phase II) before a strongly channelized, topography driven ice flow (Phase III). The latter phase is divided into several substages where the flow sets are becoming increasingly confined into the valleys, likely separated by colder, less active ice before down-melting of ice took place. A migrating ice divide and lowering of the ice surface seems to be the main reasons for these changes in ice flow pattern. Formation of ribbed moraine can occur both when the ice flow slows down and speeds up, forming respectively broad fields and elongated belts of ribbed moraines.

Keywords:

Streamlined subglacial landforms, ribbed moraine, Fennoscandian Ice Sheet, flow pattern reconstruction, deglaciation, Scandinavia, LiDAR

1. Introduction

The configuration of the Fennoscandian Ice Sheet (FIS) and its complex evolution in time and space during the Weichselian glaciation have been the subject of research for a long time (Böse et al., 2012; Hughes et al., 2016; Kleman and Glasser, 2007; Kleman et al., 1997; Mangerud et al., 1979, 2011; Svendsen et al., 2004;). This includes the discussion on the causes of the ice divide migration (Fig. 1) and the implications of this on the ice sheet dynamics, e.g. the initiation of the Norwegian Channel Ice Stream (NCIS) (Mangerud et al., 2011). The consequence of this likely lead to an enhanced drainage of large parts of southern Norway and central Sweden and a subsequent lowering the ice surface (Svendsen et al., 2015; Sejrup et al., 2009). The study area, Gausdal Vestfjell in south-central Norway (Fig. 1), is located upstream from the NCIS (Ottesen et al., 2005) and in close proximity to the later, migrated ice divide (Vorren, 1977). Such geographical setting (an inner region of the last ice sheet) also determines that this area has been one of the last parts of the FIS to become deglaciated. Therefore, it has a high importance on reconstructing the ice sheet development, glacial dynamics and the deglaciation. Numerous scientists have emphasized the significance of glacial bedforms – streamlined terrain and ribbed moraine – as the indicators of glacial dynamics (e.g. Briner, 2007; Clark, 1993, 1997; Dunlop and Clark, 2006a, 2006b; Hättestrand, 1997; Hättestrand and Kleman, 1999; Hughes et al., 2014; Knight, 2010, 2011; Roberts and Long, 2005; Spagnolo et al., 2012, 2014; Stokes et al., 2011, 2013; Trommelen and Ross, 2010). The analysis of distribution of glacial landforms on a regional scale is the primary tool for the ice flow pattern reconstructions with the so-called flowset (*ice-flow vector* by Hughes et al. (2014)) or the palaeoglacial approach (Boulton and Hagdorn, 2006; Clark et al., 2012; Greenwood and Clark, 2009a, 2009b; Greenwood et al., 2007; Hubbard et al., 2009; Hughes et al., 2014; Kleman et al., 1997; Ross et al., 2009).

The latest development within Geographic Information Systems (GIS) and the increasing accessibility of *Light Detection and Ranging* (LiDAR) terrain data have made it to be possible to create a high accuracy geomorphological maps further used for glacial reconstructions, and by so it has contributed to the development of geomorphology and Quaternary geology. The extensive mapping conducted within this study provides insight on the distribution and morphostratigraphical relationships of the glacial landforms and thus reveals new information on the glacial dynamics during the last glaciation. Based on the identified ice flow patterns, a detailed reconstruction of glacial events from the Late Weichselian and deglaciation in the Gausdal Vestfjell area are established.

2. Study area

Gausdal Vestfjell is located in Oppland County, south-central Norway, situated c. 50 km W of Lillehammer and 50 km SE of the Jotunheimen mountain region (Fig. 1). Jotunheimen is the highest part of the Scandinavian Mountains, which has functioned as one of the primary accumulation areas during the buildup of the FIS prior to the LGM (Mangerud et al., 2011). The study area shows a diverse and relatively complex topography (Fig. 1C). In general, it can be described as an undulating upland plateau, gently sloping towards the SE. The plateau is surrounded by several topographic highs, a W-E oriented mountain ridge in the N (highest peak Skaget 1685 m a.s.l.), the Kjølafjellet ridge in the SW, and the Synnfjell ridge in the SE. Within the plateau area itself, several elevated areas (1100 up to 1325 m a.s.l.) exist. Low-lying areas are commonly occupied by several natural or dammed water bodies that are linked by rivers (Fig. 1D). The two largest ones, the Fjelldokka and Etne rivers, emerge from the foothill of the northern ridge and flow towards the SE, continuing into deep glacial eroded valleys. The western border of the study area is drawn at the upper valley slope of the Rauddalen and Øystre Slidre valleys, while the eastern is along the Vestre Gausdal valley. Almost two thirds of the study area is located within the Langsua National Park and adjacent nature reserves (Fig. 1D) having different degrees of nature protection status limiting the possibilities for excavations.

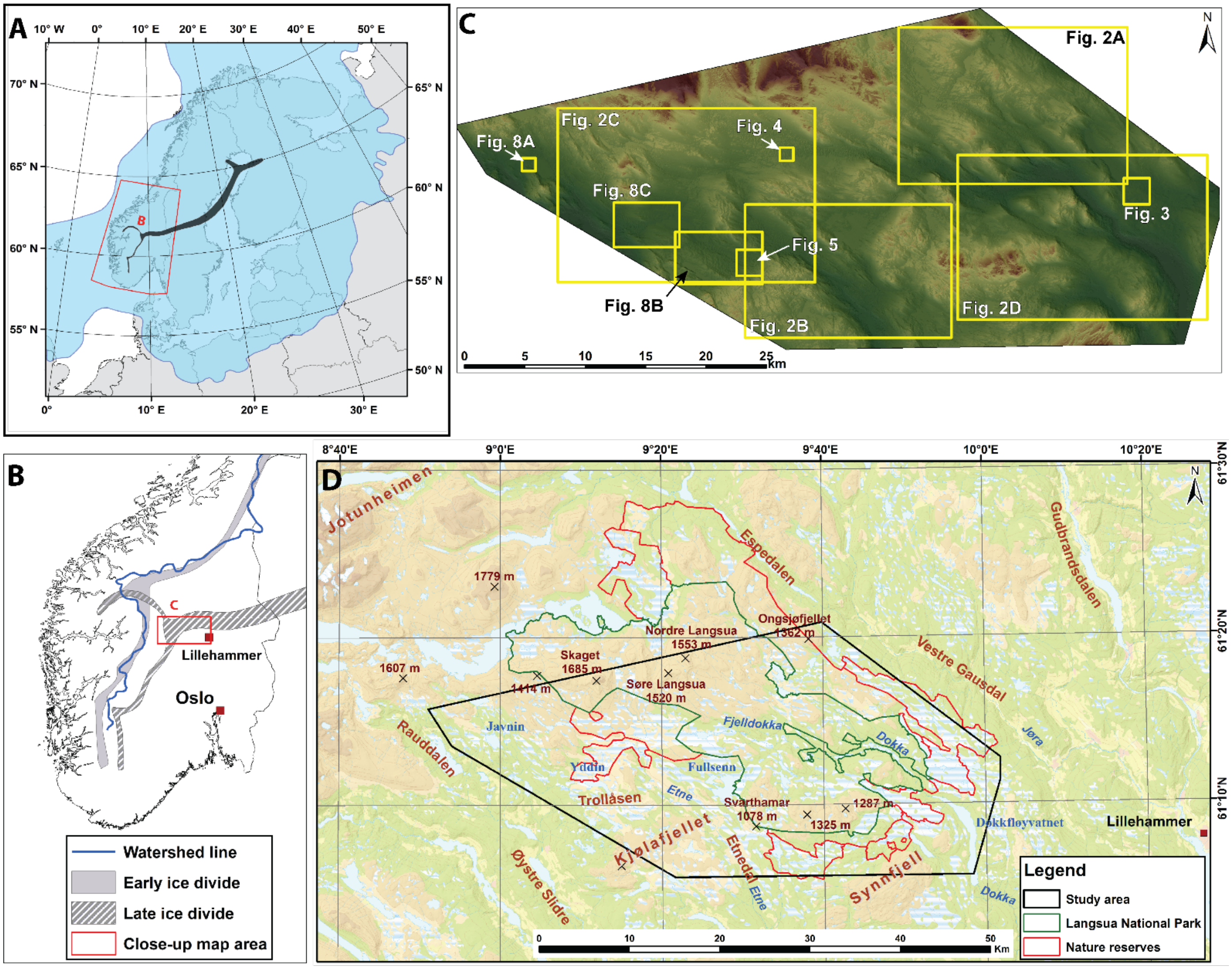

Figure 1. A. The Fennoscandian Ice Sheet at its maximum position during the Late Weichselian (according to Svendsen et al., 2004) with ice divide in dark (according to Kleman et al., 1997). **B.** Overview map of southern Norway with watershed and ice divide locations (according to Vorren, 1977). **C.** Overview map with locations of other map figures. **D.** Map of Gausdal Vestfjell with outlines of the study area and the protected Langsua National Park and nature reserve areas. Some additional location names are shown in Figs. 2 and 7.

2.1 Bedrock

The bedrock in the study area is mainly composed of metamorphosed sedimentary rocks of Precambrian to Ordovician age in nappes emplaced during the Caledonian orogeny (Heim et al., 1977). The northern and central part of the area consists of metamorphosed arkose, greywacke sandstone, and conglomerate of Late Precambrian age, and quartzite of Middle to Late Ordovician age belonging to the Jotun-Valdres Nappes Complex. In the southern and southeastern part, slate, sandstone and limestone of Cambrian to Middle Ordovician age form the Synnfjell Nappe (Heim et al., 1977). Rocks of this formation are highly deformed by faulting, thrusting, and stacking in a N-S direction and have a high degree of schistosity. In addition, there are several localities where metamorphic plutonic basement rock (metadiorite) of Precambrian age are found (Nickelsen, 1988; Siedlecka et al., 1987). These plutonic rock formations are usually found in elevation heights that stand out from the overall terrain.

2.2 Sediment cover

The sediment cover is variable in Gausdal Vestfjell due to the influence of the terrain topography as well as changes in depositional environment throughout the glacial history. Noticeably, an extensive amount of the sediment cover is made up by different till deposits that vary spatially in thickness throughout the study area (Carlson and Sollid, 1979). Deposits of continuous cover and great thickness (usually from a half to a few meters) that hide the structures of the underlying bedrock are found mainly in topographic lows and valley floors. Elsewhere (e.g. on valley sides and hilltops) glacial deposits have a discontinuous nature with frequent bedrock outcrops. Previous research on till lithology conducted in this area suggests a dominant gravely sandy matrix dominated by the local bedrock material. This suggests a short transportation prior to deposition (Carlson and Sollid, 1983). Glaciofluvial deposits, in association with landforms such as eskers, kames, deltas, and outwash fans or in form of sheet covers (related to previous meltwater basins), are widespread within the study area. There is also a common occurrence of peat and fluvial sediments deposited during the Holocene (Carlson and Sollid, 1979, 1983; Garnes and Bergersen, 1980). Sub-till sediments (glaciofluvial and glaciolacustrine deposits) of Mid-Weichselian interstadial age (Bergersen and Garnes, 1971, 1972, 1981) are found in several places in the nearby main valley of Gudbrandsdalen (Fig. 1D). However, there are no descriptions of similar findings within the study area.

2.3 Previous research

Previous reconstructions of the FIS deglaciation in the Gausdal Vestfjell area (Bergersen and Garnes, 1972, 1983; Garnes and Bergersen 1980; Olsen, 1985) are mainly based on the investigations of till deposits and glacial striations at Gudbrandsdalen and its tributary valleys (Fig. 1D). Based on their observations, Bergersen and Garnes (1972, 1983) and Garnes and Bergersen (1977, 1980) identified four phases of the last glaciation in the Gudbrandsdalen area. These are (i) *the initial phase* (ice flow followed the valleys), (ii) *the main phase* (little or no movement dependency on the topography), (iii) *later inland phase* (large variations in the directions of striae and till fabrics suggesting continuous shifting of flow directions) and (iv) *the deglaciation phase* (characterized by meltwater drainage along stagnant ice). All these phases had a predominant SE ice flow in Gausdal Vestfjell. Combining this and other research, Vorren (1977) established a unified reconstruction of the ice divide migration and the ice movement for southern Norway during the Weichselian. According to him, there are four main phases of different ice movement directions, the two youngest ones related to the Late Weichselian. The ice divide migration from the watershed region towards the E (Fig. 1B) might have happened between their Phases 2 and 3 (around 25 – 27 ka BP) (Vorren, 1977). Vorren (1977) suggests that Phase 3 should be correlated with the maximum extent of the Weichselian ice sheet (the LGM) (Fig. 1A) and with the *later inland phase (iii)* of Bergersen and Garnes (1972). Nesje et al. (1988) on the other hand, state that the ice divide migration towards the SE and E (Fig. 1B) was a result of a backward lowering of the ice sheet during the ice marginal retreat from its LGM position at the continental shelf edge to coastal and fjord areas of western Norway. Therefore, Phase 2 should represent the maximum extent of the Weichselian ice sheet while Phase 3 most likely represents a period of marginal retreat (Nesje et al., 1988). Most reconstructions of the ice divide for the entire FIS at its maximum position (e.g. Kleman et al., 1997) place it over the Gulf of Bothnia continuing westward to the eastern (late) ice divide in southern Norway (Fig. 1A). At the deglaciation, Sollid and Sørbel (1994) acknowledged a change from warm- to cold-based ice conditions at higher inland areas (such as Gausdal Vestfjell) as streamlined landforms in these areas are found together with extensive supraglacial and lateral drainage systems. Garnes and Bergersen (1980) supposed that stagnant and dead ice was located at higher elevations while active ice was flowing in the valleys as the inland ice sheet gradually down-wasted. This *deglaciation phase (iv)* of Bergersen and Garnes (1972) corresponds to Vorren's (1977) Phase 4, assigned to represent the Preboreal age (Early Holocene).

3. Materials and Methods

The glacial landforms within our study area were mapped manually using several digital input data sources. Laserscan data sets (LiDAR) provided by the Norwegian Mapping Authority (*Kartverket*) is the primary source of terrain information. Landform recognition and determination was carried out using ESRI software ArcGIS version 10.3 that supports operations with .LAS files, such as data filtering (using ground points only) and data visualizations in 3D View window. The point cloud density for LiDAR data varies in range from 10 to 100 points per square meter depending on the age of the dataset. Approximately half of the study area has data coverage with 100 DTM point cloud density (100 points per m^2). Later, for visualization purposes, a Digital Elevation Model (DEM) of 3 m horizontal resolution was processed from the LiDAR data set and a hillshade image from the DEM. Additionally, WMS servers of aerial imagery and topographic maps were used to aid the landform identification in cases of uncertainty, e.g. to exclude man-made objects like road fragments, ditches, mounds or walls. Maps of Quaternary deposits as well as various resource maps provided by the Geological Survey of Norway (NGU) were in some cases used to validate identified landforms, for example, whether a landform consist of sediments or is due to a bedrock feature. Landform's plan form in the horizontal plane were mapped based on their profile curvature and drawn along the break of a slope. A file geodatabase was established to store and organize the identified landforms (Table 1), incorporating streamlined landforms, moraine ridges (ribbed moraine), and glaciofluvial landforms. The following parameters of streamlined landforms and ribbed moraine ridges were included: landform configuration (polygon feature), axis of width (W) and length (L) (polyline features), landform type, and relative height (H) (obtained as described in Spagnolo et al. (2012)). Simple morphometric analyses of these parameters are presented in Supplement no. 1 and 3. No morphometric information was acquired for meltwater landforms (eskers and meltwater channels) as only their location in the terrain was used further in this study and due to their complex form, often consisting of more than one feature per landform. Further, interpretation accuracy of streamlined landforms (high, medium, low or not reliable at all) was added to the dataset and reassessed after field investigation. This assessment of interpretation accuracy was determined by following characteristics: (a) object size, (b) object shape and configuration, (c) structural orientation of the underlying bedrock within the area, (d) object overall location and orientation in the terrain (either on a hilltop, slope, or valley floor), (e) object relation to nearby objects, (f) possible other types of interpretation (if there is a different explanation of genesis, the reliability is decreased), (g) other aspects like sedimentary or bedrock feature. For example, distinctively shaped drumlins (located in the central parts topographic lows (valleys) or plateaus that is characterized by thick drift sheet) or small flutes overlying other landforms are regarded (in terms of accuracy) as more trustable than large-scale drumlins (crag-and-tails or rock drumlins), oddly shaped roche moutonnées located on hilltops and glacial lineations forming successive chains at valley sides, which can also be interpreted as kames.

As an important part of the study, landforms with uncertainties regarding their genesis were investigated during fieldwork. Along with the landform ground truthing, fieldwork also included collecting data on glacial striations (ten localities), as well as investigating and documenting the sediment outcrops to acquire information of internal structure and sedimentary composition of ribbed moraine ridges (eight localities) and streamlined landforms (three localities). Only two localities from ribbed moraine ridges and one from streamlined landform were further visualized and included in the paper to illustrate the sedimentary composition. A lithofacies classification modified from Eyles et al. (1983) was used in describing the sediments. Clast fabric measurements were carried out to document ice-bed stress patterns and from that deduces ice flow directions during the formation of streamlined landform. The dip and dip direction was measured for 25 matrix-supported clasts ranging from 1 to 10 cm with a/b ratio ≥1.5 (Larsen and Piotrowski, 2003). The results of the fabric measurements are presented as points and two-sigma Kamb contours on an equal-area, lower-hemisphere Schmidt net plotted in StereoNet© for Windows.

The field inspection led to an increase in the quality of acquired data and to a decreased quantity of previously identified landforms. Furthermore, the established assessment of reliability for streamlined landforms was evaluated during the field inspection. However, as field investigation is a time consuming process, and with 1190 km^2 to cover, it is impossible to fully exclude all errors in the geomorphic dataset and some of the identified landforms may have been interpreted imprecisely regarding their genesis. Only the identified streamlined landforms with interpretation accuracy assessed as high or medium of (8145 out of 9498 in total) are used for further processing (relative height estimation) and analyses within this research.

4. Results

A total of 17 164 landforms and landform features were identified and included in the database. These landforms are grouped into (a) subglacial bedforms including streamlined ridges within streamlined terrain and transverse to ice-flow moraine ridges within ribbed moraine areas, and (b) meltwater landforms including eskers, meltwater channels, kames, outwash fans and deltas (Table 1) (Fig.2). The established database is further used to analyze the spatial relations among the landforms in a manner to establish the deglaciation pattern.

Table 1. Summary of identified landforms included in database.

	Landform feature type:	**Count**	**Length (m)**			**Width (m)**			**Relative height (m)**		
			Min	Max	Mean	Min	Max	Mean	Min	Max	Mean
Subglacial bedforms	Streamlined landforms (including low or no reliability)	9547 *Further used:* **8155**	12.7	1687.8	140.8	4.12	666.2	57.7	0.2	62	4
	Ribbed moraine	3105	12.8	766.6	118.2	9.1	354.4	64.2	0.5	14.7	3.8
Meltwater landforms	Meltwater channel features	1322									
	Meltwater features (kames, outwash fans, deltas)	537									
	Eskers (lines)	2653	8.2	1685	110						
Total:		**17 164**									

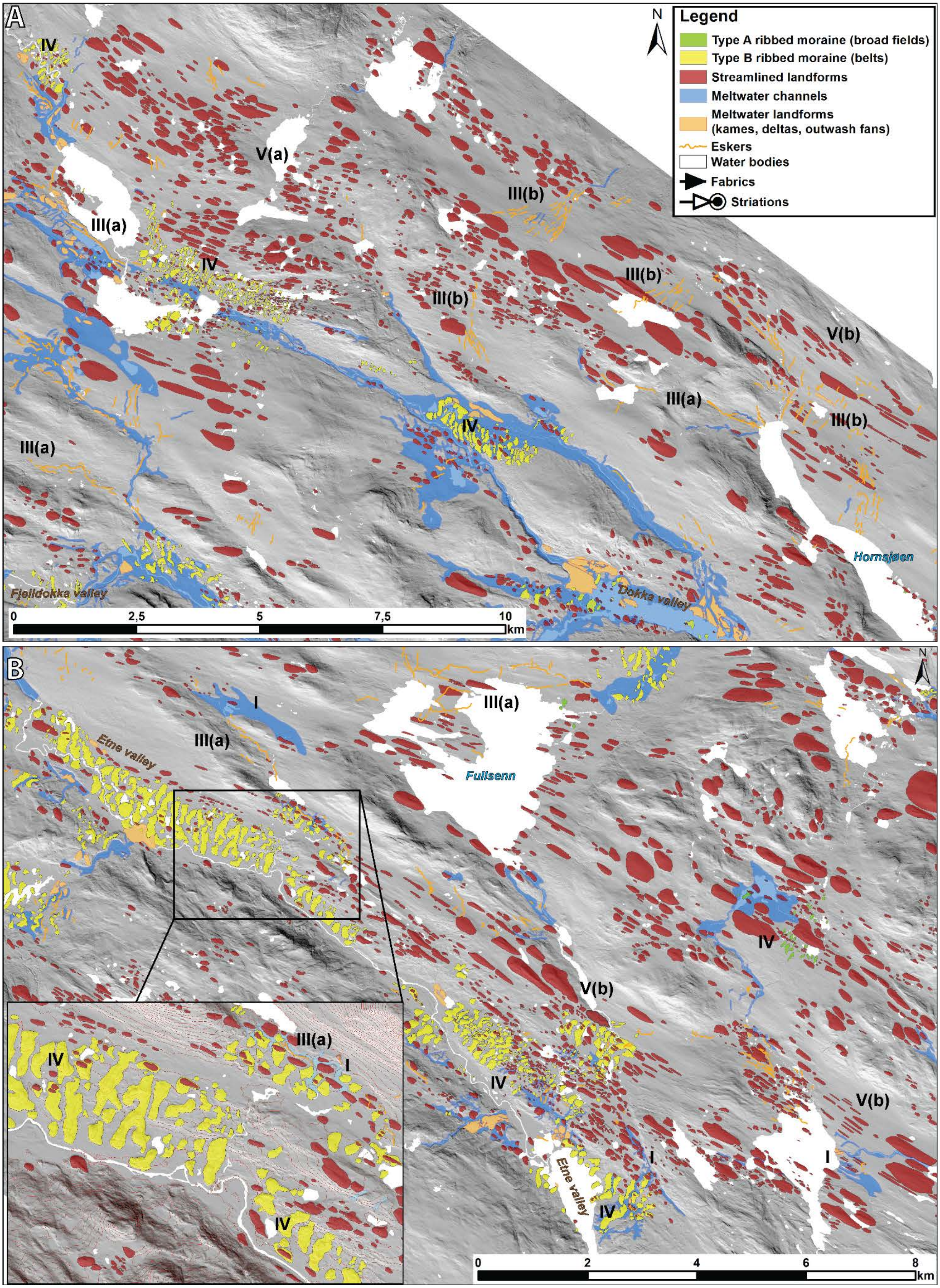
A
Legend
Type A ribbed moraine (broad fields)
Type B ribbed moraine (belts)
Streamlined landforms
Meltwater channels
Meltwater landforms (kames, deltas, outwash fans)
Eskers
Water bodies
Fabrics
Striations
N
IV
V(a)
III(a)
III(b)
IV
III(b)
III(b)
V(b)
III(a)
III(b)
IV
III(a)
Hornsjøen
Fjelldokka valley
Dokka valley
0
2,5
5
7,5
10
km
B
N
I
III(a)
III(a)
Etne valley
Fullsenn
IV
V(b)
IV
V(b)
I
I
Etne valley
IV
IV
III(a)
I
IV
0
2
4
6
8
km

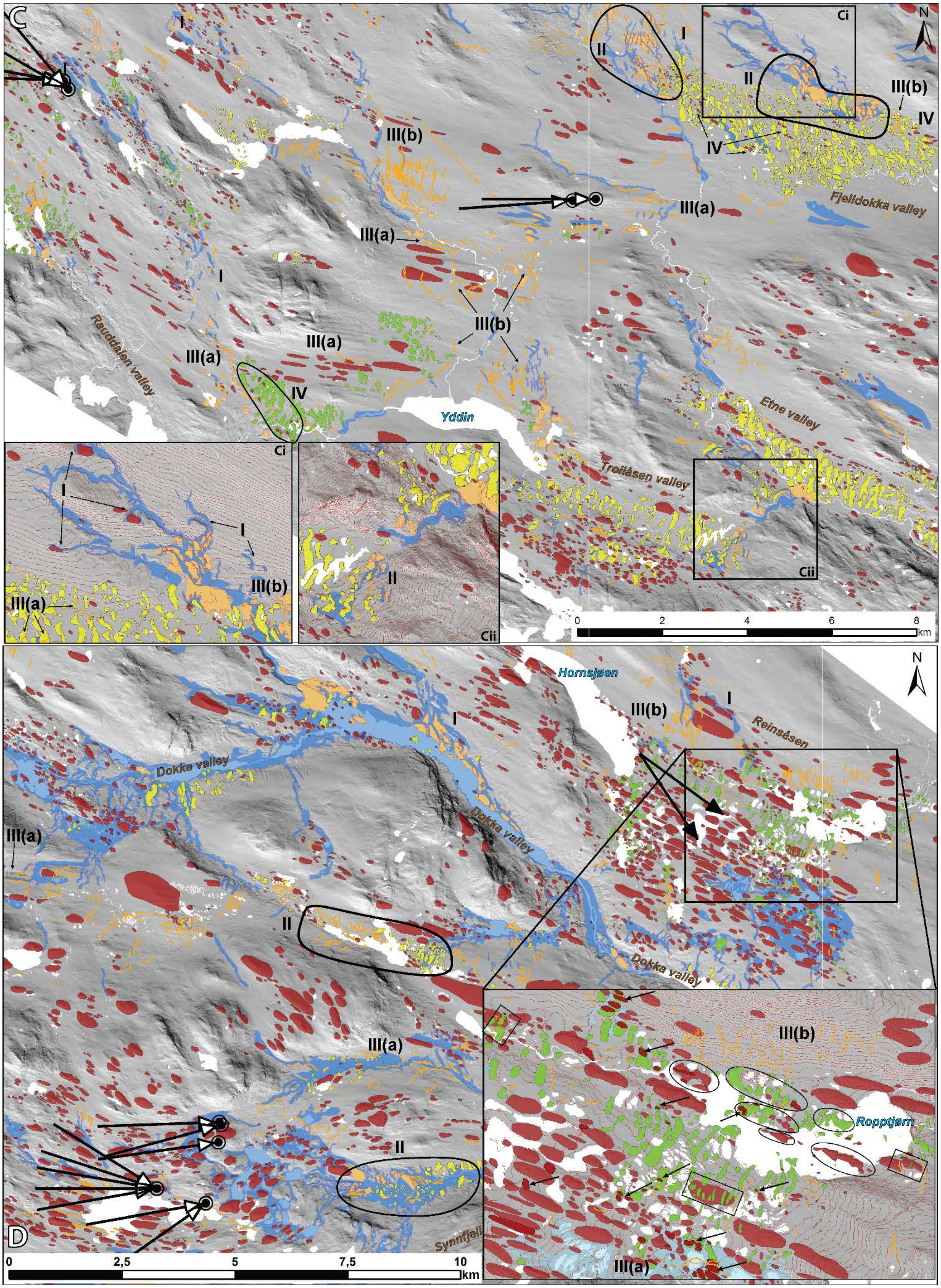

C
Ci
Cii
D
N
I
II
III(a)
III(b)
IV
Fjelldokka valley
Rauddalen valley
Yddin
Etne valley
Trollåsen valley
Hornsjøen
Reinsåsen
Dokka valley
Roppitjørn
Synnfjell
0 2 4 6 8 km
0 2,5 5 7,5 10 km

Figure 2. Distribution pattern and spatial relationships of identified landforms plotted on DEM hillshade image from four parts of the study area. See Fig. 1C for location and supplement no. 2 for a detailed map. Roman numbers indicate: (I) lateral meltwater channels; (II) close spatial relations between meltwater landforms and ribbed moraine; (III) various esker system patterns oriented (a) parallel and (b) transverse to the general ice flow direction; (IV) spatial relations between streamlined terrain and ribbed moraine ridges with streamlined landforms located both on top and in between the ribbed moraines; (V) different modes of streamlined landforms being mainly (a) round and oval shaped and (b) distinctly more elongated (L/W ratio > 3).
A. Northern part. **B.** Southern part. Close-up (5 m contour intervals) of the ribbed moraine belt (type B) in Etne valley. **C.** Western part. Close-ups (5 m contour intervals) showing (Ci) meandering lateral meltwater channel (I) and (Cii) ribbed moraine and meltwater landform spatial relations (II). **D.** Eastern part. Close-up (2.5 m contour intervals) of a broad ribbed moraine field (type A) from the plateau S of Reinsåsen with various modes of the streamlined landforms transforming into ribbed moraines. Reworked streamlined landforms in circles, overlying ribbed moraines in boxes, and the smaller streamlined landforms with varying orientation partly overlying ribbed moraine and older streamlined landforms marked by arrows.

4.1. Subglacial bedforms

4.1.1. Streamlined landforms

For simplicity, we use the term ‘streamlined landforms’ in this paper to refer to the broad family of glacially streamlined terrain landforms including flutes, drumlins, rock drumlins, crag-and-tails, roche moutonnées and glacial lineations (as defined by Stokes et al. (2013)). This use is without restricting the variety of their shape and size or without unambiguously linking them to a certain formation mechanism as the only plausible cause. The 8155 identified streamlined landforms classified with medium or high reliability, have morphological parameters varying within a wide range (Table 1). The relative height varies from 0.2 m up to 62.2 m. However, there is only one feature higher than 50 m while 13 others are forming a cluster around 40 m (see supplement no. 1). This suggests that the highest landform is an outlier and is thus excluded as unrepresentative, resulting in a change of the interpretation accuracy class of this particular landform to ‘low’.

Streamlined landforms are found at various elevation levels throughout the whole study area (Fig. 2, supplement no. 2). The most prominent (widest and highest) ones are often situated in close relation to local topographic bumps (Fig. 2A, supplement no. 3), and therefore indicating either the importance of bedrock presence (rock core), or a diminished streamlining due to the lack of sediment or porewater, or a combination of both at their formation. Less distinct (lower and narrower) streamlined landforms are located on slopes and topographic lows (Fig. 2, supplement no. 3). It is in this setting that the most elongated ones (L/W ratio > 3) often appear located on the shadow (lee) side of larger topographic bumps throughout the study area (Fig. 2A and B). The majority of such more elongated features are located either around Etne valley (Fig. 2B) or in the eastern part of the study area (Fig. 2D). The smallest of the identified streamlined landforms are often found in close association with ribbed moraine, either on top of ridge crests or between them (Fig 2B and C, supplement no. 2).

Only a few outcrops of the streamlined landforms are available in the study area. At Reinsåsen (Fig. 2D and 3), the uppermost 2 m of the middle of a drumlin consists of compact, matrix-supported diamicton with numerous cobbles and boulders. The diamicton is in the upper ca. 1 m sandy while it is silty sandy below. Clast orientations are strong (S_1 = 0.87 and 0.89) indicating a depositional stress transfer towards SE and SSE (Fig. 3). A 5-15 cm thick massive, sandy silt lens is found within the diamicton. The diamicton at Reinsåsen is interpreted as a subglacial traction till due to its compact, unsorted character and strong fabric orientations (Evans et al., 2006) where the fabric analyses suggest ice movement towards SE, slightly more southerly directed than the orientation of the drumlin. The two other investigated exposures are as well in drumlins revealing similar compact, matrix-supported sandy diamicton, also interpreted as subglacial till.

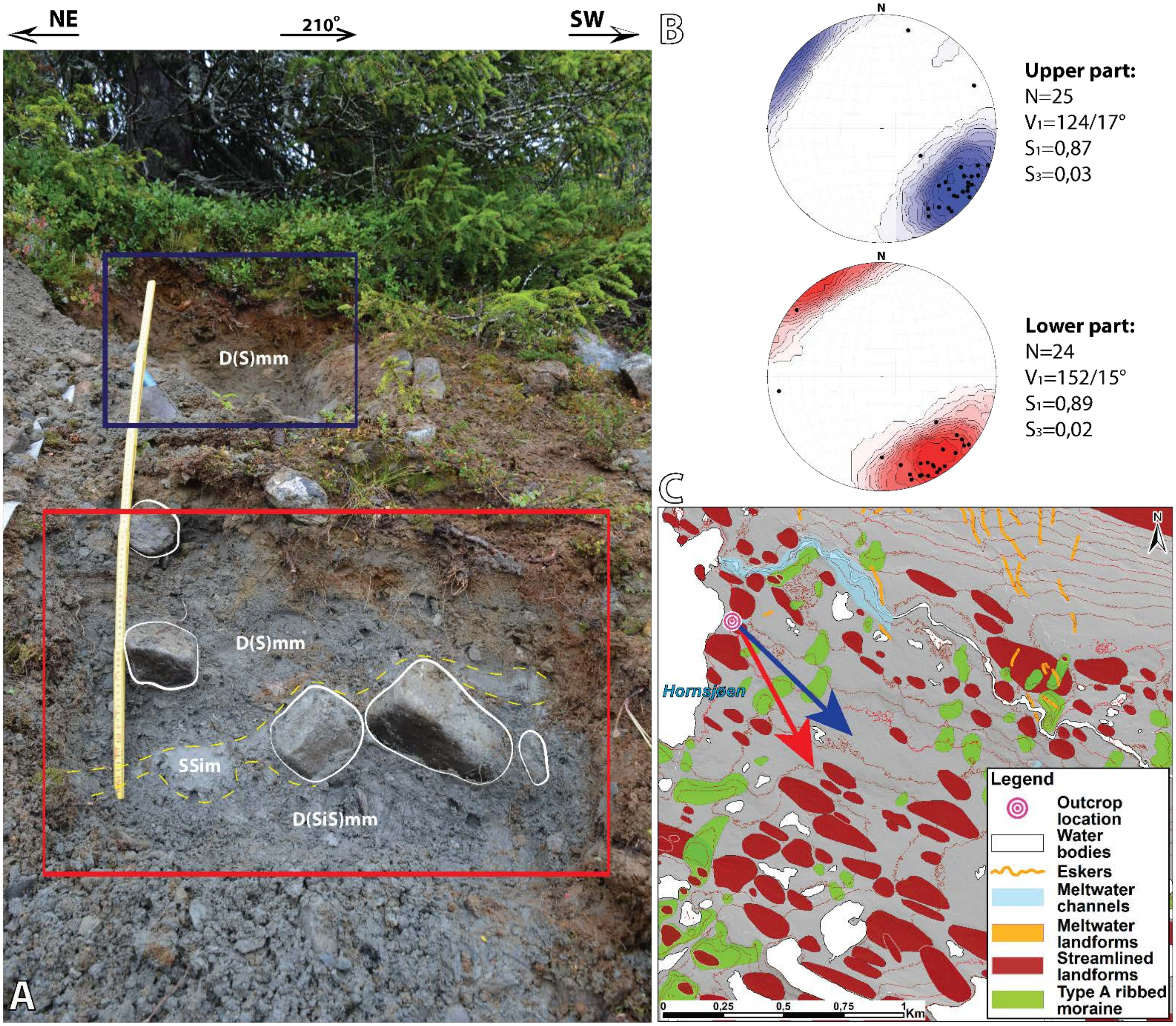

Figure 3. Sediment outcrop near the top of a streamlined landform (drumlin) at Reinsåsen located on the plateau S of the lake Hornsjøen. **A**. Photo of outcrop (scale 1 m long) with identified lithofacies (for lithofacies code descriptions see Table 2), stippled lines outline sediment boundaries. The boxes represent the parts where fabric measurements were taken. Color code: blue – upper part, red – lower part. **B**. Contoured stereoplots of clast fabric measurements. **C.** Glacial landform map of the Reinsåsen area (2.5 m contour intervals). Colored arrow lines represent the ice flow direction as interpreted from fabrics measurements. Note the overlying landforms: smaller streamlined landforms and eskers on top of both ribbed moraine ridges and larger streamlined landforms, and ribbed moraine ridges on top of larger streamlined landforms.

Table 2. Overview of the lithofacies code used to describe the outcrops. Modified from Eyles and others (1983), following Möller (2005).

Lithofacies code	Lithofacies type description: grain size, grain support system, internal structures
D(G/S/Si/C)	Diamicton, gravely, sandy, silty, clayey. One or more grain-size code letter used in brackets
D( )mm	Diamicton, matrix-supported, massive
D( )ms	Diamicton, matrix-supported, stratified
GSm	Gravely sand, massive
Sm	Sand, massive
SiSm	Silty sand, massive
SSim	Sandy silt, massive
GSpc	Gravely sand, planar cross-laminated
Spc	Sand, planar cross-laminated

4.1.2. Ribbed moraines

A total of 3105 features were identified as ribbed moraine ridges, and taken into account for analysis. The morphological parameters (length, width, relative height) of the ridges varies within a broad range (Table 1). There are no obvious outliers and the data show relative homogeneity of height distribution (supplement no. 1).

It is observed that moraine ridges either tend to be agglomerated into broad fields, our type A ribbed moraine area (Fig. 2D), or elongated belts located on the valley floors, our type B ribbed moraine area (Figs. 2B and C). The type A ribbed moraine is seen preferentially in the eastern part of the study area, while type B ribbed moraine is found throughout the whole study area (Fig. 2). Ribbed moraine ridges of type A are considerably smaller in geometry (length and width, and the relative height) than type B (Fig. 2B). The distance between the ribbed moraine ridge crests (or the 'wavelength' proposed by Dunlop and Clark, 2006b) tend to be wider for type A. Moraine belts are from around 2 km up to 16 km in length and, on average are around 1 km wide. Noticeable ribbed moraine belts are located in Fjelldokka (755 features, Figs. 2C and 4) and Etne valleys (Fig. 2B), and the ridges there tend to have the highest relative heights and largest width and length parameters of all the identified ribbed moraines. The most distinct ridges are located in the middle parts of all the ribbed moraine belts (supplement no.3).

The few investigated sediment outcrops from the ribbed moraine ridges reveal a relatively complex inner structure that consist of both diamictons and sorted sediments, of which two localities are briefly presented here. The section at Haldorbu in the Fjelldokka valley (Fig. 4) is 2-3 m high and 10 m wide, and is oriented almost perpendicular to the ridge at its proximal side. Numerous cobbles and boulders are found scattered in compact, massive matrix-supported sandy diamicton in the uppermost 1 m. Some of the larger clasts, as well as lenses of massive silty sand and gravelly sand are tilted towards W. The diamicton is set through by several shear planes, also dipping towards W. The lower part of the exposed section is dominated by layers of massive sand and planar cross-laminated sand and gravelly sand. These sorted sediments are partly deformed by shear planes and flame structures, and by bifurcating intrusions of massive, matrix-supported sandy silty diamicton. At the second site, the uppermost 1 m of the proximal side of a ridge at Trollåsen (Fig. 5) is dominated by compact, massive matrix-supported sandy and silty sandy diamicton, slightly coarser and more consolidated than the diamicton at Haldorbu. Close to the surface, stratified matrix-supported gravelly sandy diamicton is common. Many of the abundant cobbles and boulders are orientated parallel with the ridge surface (tilted towards W), a similar orientation that is also displayed by the numerous shear planes cutting the diamicton and some few lenses of massive silty sand.

The diamicton at both Haldorbu and Trollåsen is interpreted as a subglacial till based on its compactness and glaciotectonic structures as shear planes (Evans et al., 2006). The sorted sediments at Haldorbu must have another origin as e.g. lacustrine or fluvial before being deformed, likely by an overriding glacier. The intrusions at Haldorbu are interpreted as clastic dykes suggesting, together with the presence of flame structures, depositional conditions with a high water saturation and overloading (Damsgaard et al., 2015; Le Heron and Etienne, 2005; van der Meer et al., 2009).

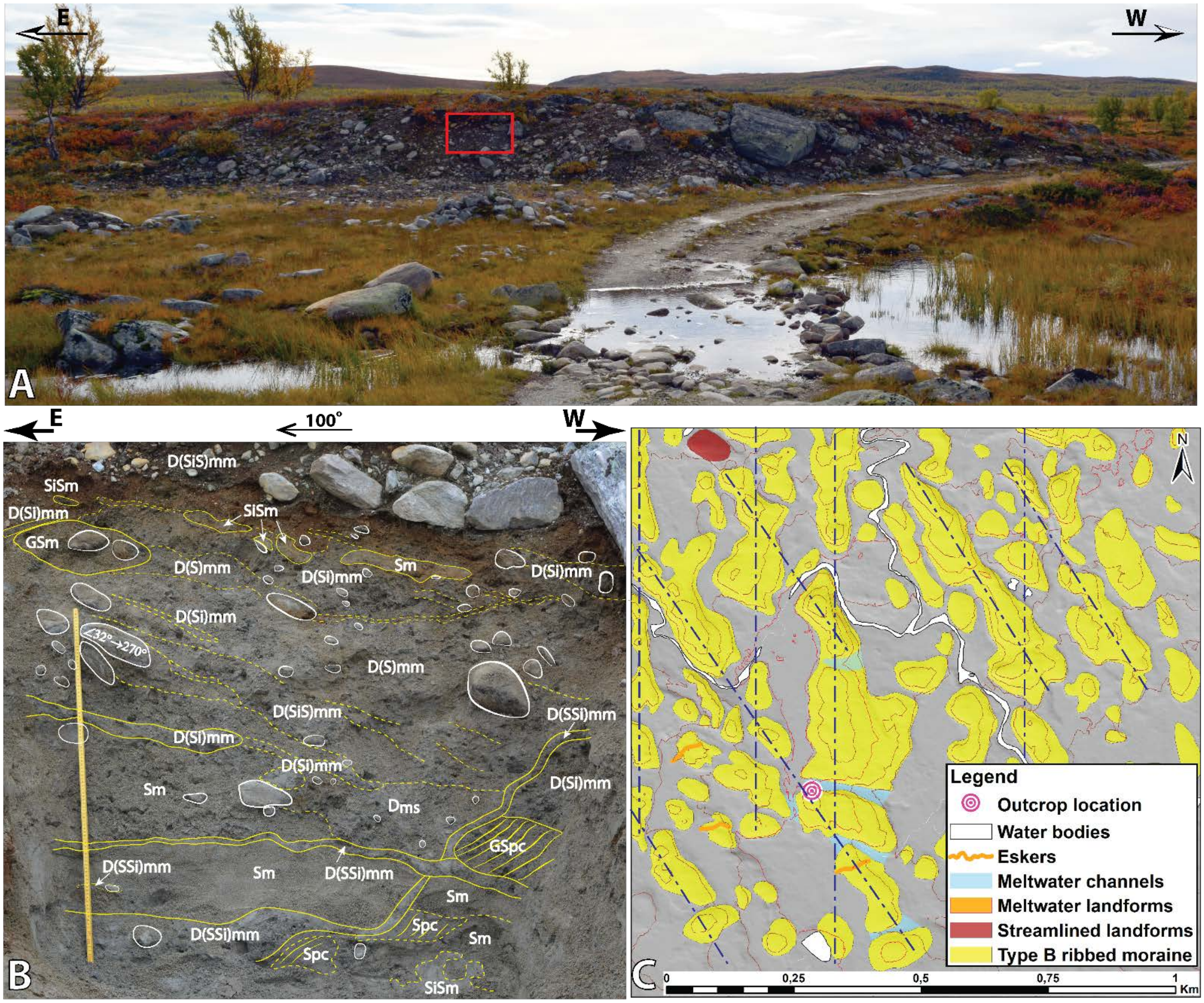

Figure 4. Sediment outcrop at the proximal side of a moraine ridge near Haldorbu, in the Fjelldokka ribbed moraine belt. **A.** Overview photo of the outcrop. The outcrop is partly natural, located on the side of a meltwater channel. **B.** Close-up photo (scale 1 m) of investigated part of the outcrop (red box in A) with lithofacies (see Table 2). Stippled lines mark sediment boundaries and glaciotectonic features. Note the cross-cutting clastic dykes filled with sandy silty diamicton. **C.** Glacial landform map from the nearby area of the outcrop (2.5 m contour intervals). Note the eskers on top of and meltwater channels cross-cutting the identified ribbed moraine. Stippled lines mark the two orientations of the ribbed moraine ridges; see Fig. 2C for larger coverage area.

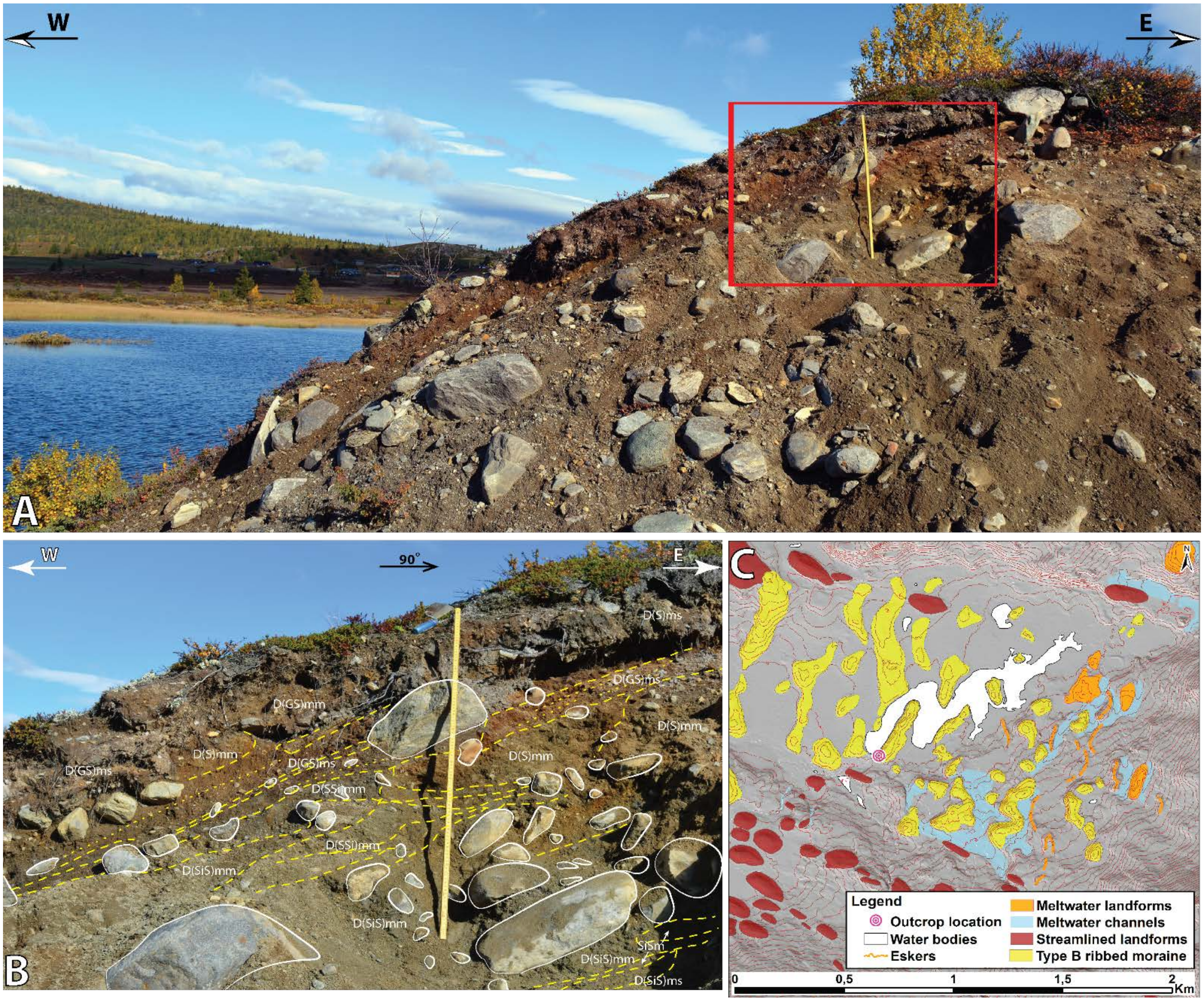

Figure 5. Ribbed moraine ridge in the Trollåsen area. **A.** Overview photo of outcrop (scale 1 m), situated in proximal side of the landform. **B**. Close-up of investigated part (box in A) with identified lithofacies (see Table 2). Stippled lines mark sediment boundaries and glaciotectonic features. **C**. Glacial landform map of the nearby area (2.5 m contour intervals). Note the spatial relation between and orientation of identified ribbed moraine ridges and meltwater landforms, orientation of these ridges are similar indicating perpendicular direction of respectively ice flow and meltwater flow.

4.1.3. Spatial relations of glacial landforms

The mapping of glacial landforms in Gausdal Vestfjell suggest some correlations between identified landforms regarding the size, morphology and their overall location in the terrain, as well as spatial relations between streamlined landforms and ribbed moraine ridges. Both types of landforms indicate a dominant ice movement towards the SE at their formation.

There are two spatial distribution types of ribbed moraine (see also 4.1.2), broad fields (type A) and elongated ribbed moraine belts (type B). Type A ribbed moraine (broad fields) are occurring more sparsely and are generally located in open areas not constrained by the topographical conditions (Fig. 2D). Ribbed moraine of this type occur at the same topographical level as the surrounding streamlined landforms. Type B ribbed moraine (belts) areas host the most pronounced ridges and are mainly found at lower hypsometric levels than the surrounding streamlined landforms (Figs. 2B and C, supplement no.3). Ribbed moraines of this type are usually located in confined elevation lows (narrow valleys) that are often followed by an increasing slope gradient in ice flow direction. Ribbed moraine areas of both types are often followed by distinct and well-elongated (L/W ratio >3) streamlined landforms further down-flow (as seen distinctly in Fig. 2B). As noted in 4.1.1, the size and shape of streamlined landforms varies regarding their elevation in the terrain, and their divergence in orientation occur at varying elevation heights (Fig. 2, supplement no. 2 and 3).

Both ribbed moraine ridges and streamlined landforms are often found in superposition, in some cases with diverging orientations and sometimes showing signs of re-molding. Found within the whole study area, although more abundant in the eastern part, are smaller streamlined landform overlying other streamlined landforms with a different orientation indicating a change in ice flow direction (Figs. 2D and 3C). Some moraine ridges within type B areas are similarly found with diverging orientations (Fig. 4C). The streamlined landforms are often located in close association with ribbed moraines of both types, being more abundant within the ribbed moraine belts (type B). In these cases, the streamlined landforms are located either on top of the ribbed moraine ridge crests or in between them, and are usually small in size (IV in Fig. 2). We suggest that this morphostratigraphical relation show a transition in landform build-up from transverse- to parallel-to-ice-flow as a continuous change with time at the same glacial events. In addition, we have also noticed the reverse – a transition from streamlined landforms into ribbed moraines at several localities, mainly within the broad fields of ribbed moraine (type A). Two types of morphostratigraphical relations are observed, deposition of moraine ridges on top of streamlined landforms (Figs. 2D and 3C) and a distinct fragmentation of streamlined landforms where the landform is converted into moraine ridge by re-shaping the bulk of landform (Fig. 2D close-up).

4.2. Meltwater landforms

Several meltwater landforms like meltwater channels, eskers, kames, deltas, and outwash fans (Table 1) are identified within the study area. Although this genetic group of landforms is not in the primary scope of this study, it is an important source of additional information in regards to deglaciation patterns of the study area. Identified meltwater landforms are often found on top of (eskers) or cross-cutting (meltwater channels) both ribbed moraine ridges and streamlined landforms (Figs. 2, 3C, 4C and 5C) suggesting that they were formed at a later stage than the glacial landforms, likely during the deglaciation of the area.

Two groups of distributional pattern of eskers are recognized, parallel (III(a) in Fig. 2) and transverse (III(b) in Fig. 2) to the general ice flow direction. Eskers of the first group usually form longer and more distinct systems, thus suggesting they evolved over a longer period of time, while the others form shorter systems and have more fragmented characteristics indicating shorter time of development. Judging from the morphology and location on the valley slopes, it is reasonable to assume that the transverse eskers (III(b) in Figs. 2A and D) were formed at the very last stages of deglaciation when dead ice was heavily crevassed, meltwater fluxes were high, and plenty of sediments were accessible (c.f. Garnes and Bergersen, 1980). Field observations suggest that some of these features (II in Figs. 2C and D) formed in open supraglacial channels as crevasse fill as areal down wasting of the ice occurred.

Numerous eskers and meltwater channels have close spatial relations with each other (Fig. 2) suggesting a highly connected meltwater drainage system, and that there was a spatial evolution from a subglacial to proglacial environment. Most of the identified meltwater channels are lateral channels and reveal complex development during the deglaciation (Fig. 2, especially close-up Cii). When in close proximity to eskers, some of the meltwater channels have been found to be (a) continued by an esker (NW in Fig. 2B), (b) located downstream from an esker (N in Fig. 2A), or (c) contain esker features within the channel (Fig. 2D), thus having a clear subglacial origin at least for the initial part of the landform formation.

Often meltwater channels and eskers are in their distal down-flow direction connected with deltas, outwash fans, or kames of various shapes and sizes. In some cases, like in the Fjelldokka valley, deltaic and outwash fan features are found close to the valley sides where their morphology appears similar to the nearby ribbed moraine (Figs. 2C and 5C). This suggests that these outwash fans were accumulated in ice crevasses in a very late phase, burying the underlying ribbed moraines. In other cases, as for Etne valley, outwash fans are deposited partly over and in between several ribbed moraine ridges (Figs. 2B and C), suggesting at least partly ice-free conditions.

4.3. Bedrock influence and striations

Bedrock topography have evidently a large influence on the depositional pattern of glacial sediments as a majority of the observed subglacial landforms and meltwater features in the study area are located either (sub-) parallel or transverse to the valley trends, that follow the structures and weakness zones of the bedrock. Hilltops have often acted as obstacles. Several locations of glacial striated bedrock are found in the study area. Although the direction of the measured striations varies locally, the ice flow direction dominantly indicated from striae is towards the SE and E. This is a general directional trend throughout the whole study area. Often the measured azimuths coincide with the orientation of the crests of streamlined landforms on which the striations are found (Fig. 6).

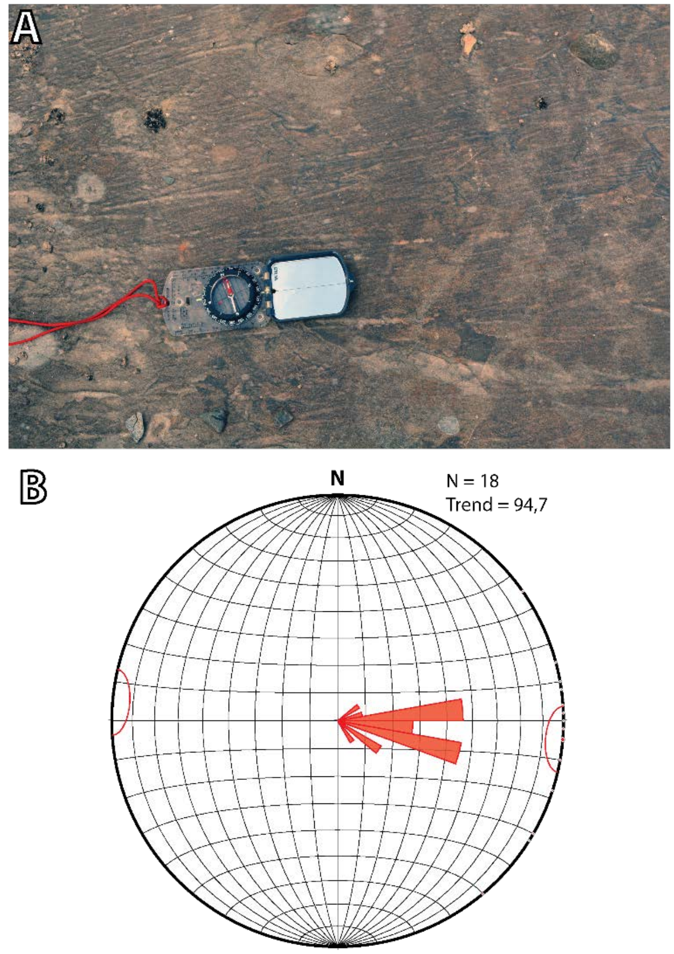

Figure 6. Overview of bedrock striations within the study area. **A.** Striations on meta-sandstone outcrop from valley N of Synnfjell. **B.** Rose diagram of measured striation azimuths. See Fig. 2 for striae measurement locations.

5. Flow patterns

In the study area, the orientation of identified streamlined landforms and ribbed moraine ridges (Fig. 7A) are the main indicators of former ice-flow direction, and therefore the primary basis for differentiating changes in the ice flow over time. The spatial and morphostratigraphical relations between these landforms, such as cross-cutting, overlying and reworked landforms (as seen in e.g. Figs. 2D, 3C and 4C), are subsequently used to reconstruct a sequence of flow patterns. For the latter we also used the altitudinal occurrence of these landforms in the terrain, as we consider landforms at higher altitudes to be older than those at the lower positions. This is based on that south-central Norway, including Gausdal Vestfjell, underwent a vertical thinning of the ice sheet during the deglaciation (Garnes and Bergersen, 1980; Sollid and Sørbel, 1994). Meltwater channels and eskers are here used as an additional information source for flow pattern reconstruction, especially for the later stages of flow prior to the deglaciation. The identified flow pattern within the study area (Fig. 7, supplement no. 2) is characterized by an overall tendency of diverting a general SSE oriented flow (phase I) into a more localized (phase II) flow towards the SE, which is then developed further into several superimposed channelized flows (phase III).

Phase I or *the topographically independent phase* is the earliest glacial phase that is identified within the study area (Fig. 7B, supplement no. 2). It is represented by the streamlined landforms that are found at high elevation levels, on the erosional plateau hilltops as well as the hilltops on the northern border of the study area. This phase has a distinct signature of SSE ice flow direction.

The following phase – phase II, is called *the regional flow phase* due to its well-developed flow pattern (Fig. 7B, supplement no. 2). Most of the identified streamlined landforms represent this phase, and come in a large range of sizes. Broad fields of ribbed moraine (type A) are characteristic to this phase, and are overlying phase II streamlined landforms. Phase II has a very distinct SE flow direction pattern that coincides with the general elevation slope in the area.

The youngest identified phase is phase III, called *the channelized flow phase*, displaying an increased topography control over the ice flow (Fig. 7C, supplement no. 2). It is characterized by a landform-complex of ribbed moraines (type B), streamlined landforms and meltwater features. The ribbed moraine tend cluster in belts, while other areas are dominated by distinctly elongated streamlined landforms as well as smaller streamlined landforms overlying ribbed moraine ridges (Figs. 2 and 7C, supplements no. 2 and 3). Parallel esker system are commonly found close to the onset of phase III flow sets. The geological record shows a complex sequence of events, where several substages are distinguished (Fig. 7C). We have to note that it is difficult to estimate the relative age relations between the different flow sets of phase III as overlying relation do not exist in or between some areas. This is especially true for the western part of the study area as the flow pattern here belonged to the system in the Øystre Slidre valley (Figs. 1C and 7C), which is only partly covered in this study. Therefore, the distinguished substages of phase III are mainly based on observations from central and eastern part of the study area. In some areas, the flow sets are parallel and overlapping each other, making it hard to distinguishing them. Here we only mark the latest imprint of flow that are identified (Fig. 7C).

Streamlined landforms representing the pre-early phase III are identified in the northern part of the study area (Fig. 7C). From the mountain ridge, the flow sets widens and display a slightly divergent flow. These landforms are found in a close relation to landforms of phase II, but must be younger as they are overriding phase II landforms and have an offset in the flow direction with a more easterly orientation. The relative age estimation is further constrained as early phase III ice flow is found cross-cutting the pre-early phase III flow set located to the NE.

The flow patterns of early phase III are distinguished in several places and mainly at high elevations within the study area (Fig. 7C, supplement no. 2). The streamlined landforms found there are often small and less elongated, and tend to be directed downwards into the valleys where a distinct flow pattern of a younger age (middle phase III) is found, and partly cross-cutting. This suggests a continuous transition into flow pattern of the younger middle phase III.

The middle phase III flow sets are found at lower elevation levels than the features of the early phase III flow, and is characterized by streamlined landforms of various sizes with a few narrow ribbed moraine ridges that are overridden by smaller streamlined landforms. During the middle phase III substage, the main ice flow drainage in the eastern part occurred through the valley N of Synnfjell and the Fjelldokka – Dokka valley and its tributaries (Fig. 7C, supplement no. 2). The flow diverted into the deepest part of the valley, however, as the same route was also used after a gradual transition into the late phase III it is difficult to differentiate between the middle and late substages in these areas. In the Fjelldokka – Dokka valley system, two ice flow patterns of middle phase III age are distinguished in different hypsometric levels, representing the early (wider flow set located higher up and is overriding the topographic obstacles) and late (flow set located lower in terrain and in lee side of topographic obstacles) part of this substage. The flow system from Etne valley to the valley N of Synnfjell likely commenced at this substage, partly cross-cutting early phase III flow diverting into the valley.

The flow pattern of late phase III age is represented by the variety of streamlined landforms, ribbed moraine ridges and smaller streamlined landforms overlapping the ribbed moraine. These landforms are found in the lowest areas of the terrain, the valley floors, and it can be traced extensively through the whole study area (Fig. 7C, supplement no. 2). This includes the Fjelldokka – Dokka valley and its tributaries where it can be traced up to the northern mountain ridge, and the valley N of Synnfjell and Etne valley in southern part.

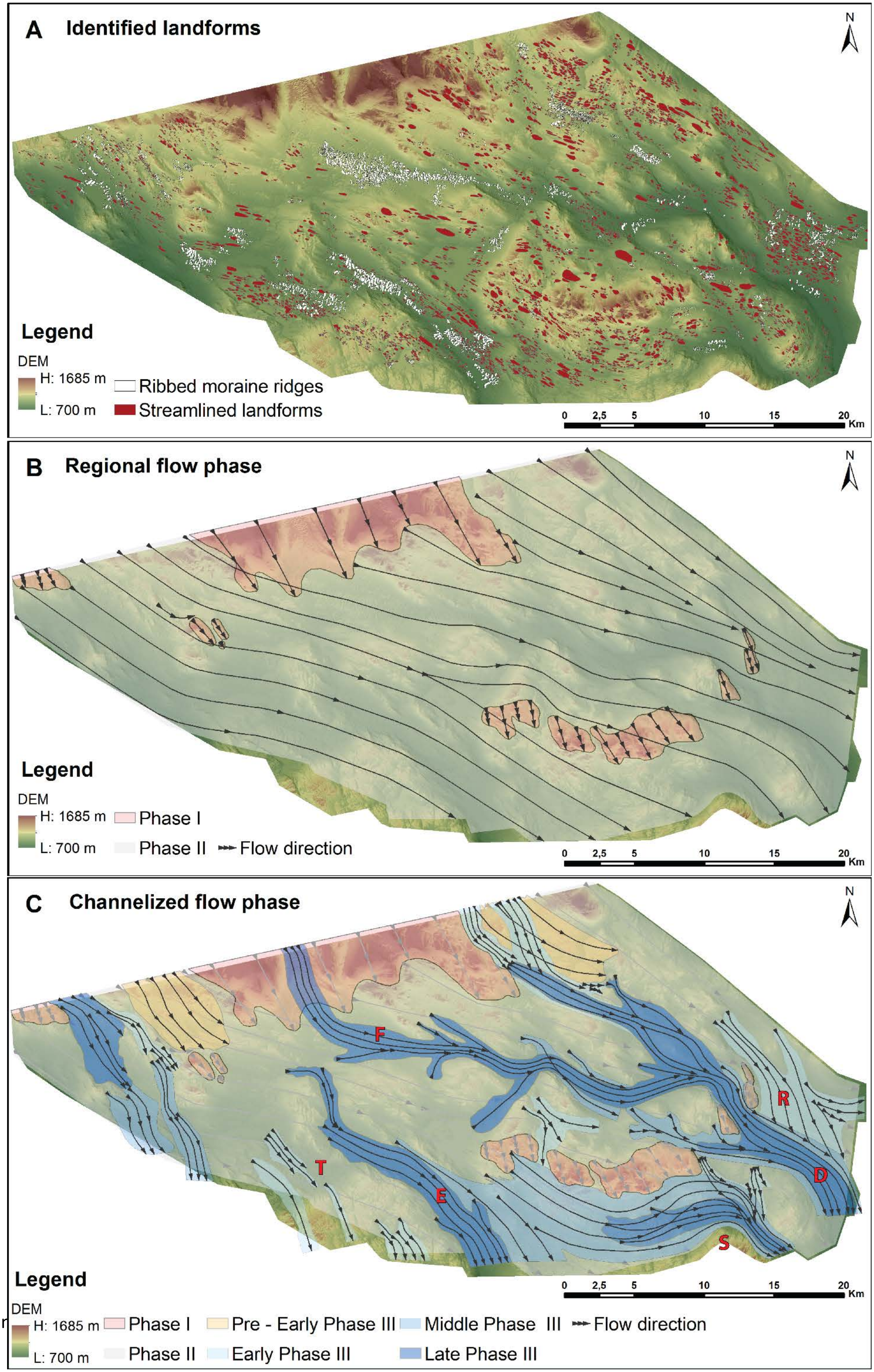
A Identified landforms
N
Legend
DEM
H: 1685 m
L: 700 m
Ribbed moraine ridges
Streamlined landforms
0 2,5 5 10 15 20 Km
B Regional flow phase
N
Legend
DEM
H: 1685 m
L: 700 m
Phase I
Phase II
Flow direction
0 2,5 5 10 15 20 Km
C Channelized flow phase
N
F
R
T
E
D
S
Legend
DEM
H: 1685 m
L: 700 m
Phase I
Phase II
Pre - Early Phase III
Early Phase III
Middle Phase III
Late Phase III
Flow direction
0 2,5 5 10 15 20 Km

Figure 7. Reconstructed ice flow pattern. **A.** Identified glacial landforms used for the flow pattern reconstructions. **B.** The early development of flow patterns (phase I and phase II) dominated by regional, topography-independent ice flow. **C.** Late-stage flow pattern (phase III and its substages) with channelized ice flow characteristics. For explanation, see text. Letters indicating place names mentioned in text: T – Trollåsen, F – Fjelldokka valley, E – Etne valley, S – Synnfjell, R – Reinsåsen, D – Dokka valley. See supplement no. 2 for a detailed map.

6. Discussion

6.1. Glacial development

The reconstructed ice flow sets in Gausdal Vestfjell show a general SE orientation of ice flow. Phases II and III (including all substages) display an increasing dependence on topography, becoming more and more confined to lower elevated areas as well as an increased interaction with meltwater features. None of the ice flow phases are dated, but due to the relatively fresh appearance and extensive preservations of the identified glacial landforms as well as the gradual transition development of phases II and III and the following deglaciation, we assume they are from Late Weichselian and the following deglaciation by down wasting. However, an older age of phase I cannot be excluded.

Phase I. Our phase I with topographically independent ice movement towards SSE is previously described as *the main phase* by Bergersen and Garnes (1972), and noted by Sollid and Sørbel (1994). It is a prerequisite to have had warm-based and sliding ice conditions under which the streamlined landforms formed. The ice sheet thickness must have been considerable to overcome the topographic obstacles as ice flowed over the mountain Skaget at an altitude of 1685 m a.s.l. This is in accordance with Mangerud (2004) and Olsen et al. (2013), reasoning that the ice thickness was >2000 m a.s.l. The FIS surface probably covered all the peaks in southern Norway (Goehring et al., 2008; Mangerud et al., 2011), although this has been debated (Mangerud et al., 2011; Nesje, 1992; Nesje et al., 1988). Olsen et al. (2013) argue that the LGM maximum ice thickness of western FIS was reached prior to 26 ka (LGM 1) when the ice divide was located at its western position (Fig. 1B). As phase I indicates the thickest ice over Gausdal Vestfjell and with an ice divide to the NW, it may represent this western FIS maximum. However, it is also possible that phase I is from a previous glaciation, at least some of the more bedrock-dominated landforms could have be formed cumulatively over several glaciations (cf. Fig. 3 in Fredin et al., 2013).

Phase II. The morphological features of Phase II (regional ice flow) consist of the majority of all identified streamlined landforms, including some of the largest and most elongated landforms. Their spatial orientation suggest a well-developed flow pattern following the general topography towards SE with some deflection around the higher mountain ridges (Fig. 7B). This points towards a relatively long-existing phase of warm-based ice as the most pronounced and elongated subglacial landforms are considered to have been formed during a longer period than smaller features (Fowler et al., 2013) and to a thinner ice, slightly more affected in its flow pattern by the underlying landscape. The onset of the vertical thinning in the Gausdal Vestfjell area may have occurred at the same time as at the mountain Blåhø (1617 m a.s.l.), situated ca. 70 km N of the study area, soon after 25.1 ± 1.0 ^{10}Be ka (Goehring et al., 2008). Several authors (e.g. Dahl et al., 2010; Mangerud, 2004; Olsen et al., 2013) have suggested that the ice surface lowering may have had a significant contribution of an active operating NCIS, effectively removing ice from the interior areas. If this is correct, then the lowering seen in phase II must have happened before ca. 17 ka at which time the Norwegian Channel was completely deglaciated (Sejrup et al., 2009).

Phase II with its abundance of streamlined landforms can be correlated to Phase 3 by Vorren (1977) and (together with phase III) to the *later inland phase* by Bergersen and Garnes (1972), characterized by its continuous shift of flow directions. Vorren (1977) suggested his Phase 3 represented the FIS maximum extent with an ice divide at its easternmost position (Fig. 2B). We consider a LGM age of phase II as plausible, however, there may have been (periods of) prevailing cold-based conditions beneath the ice divide during the LGM, similar to the cold-based preservation zones in central Sweden (e.g. Kleman et al., 1997). No positive indicators, such as block fields, are found in the study area although there are several nearby, slightly N and W of the late ice divide (Olsen et al., 2013). Phase II can possibly represent a later stage of the LGM, perhaps even closer in age to the deglaciation in line with the apparently gradual transition from phases II to III and to the following down-wasting (Garnes and Bergersen, 1980). Irrespective of age, as phase II in Gausdal Vestfjell displays an unambiguous ice flow towards SE, the ice divide must have been to the NW. This suggest that close to the study area, the ice divide was located at a more westerly position, at least as far W and N as possible within the late ice divide zone by Vorren (1977) (Fig. 1B). At some locations, the phase II streamlined landforms are overlaid by broad field type A ribbed moraines with the similar regional flow pattern (Figs. 2 and 3C). This depositional shift from streamlined landforms to ribbed moraine suggest that the ice velocity slowed down at the late part of phase II (Hall and Glasser, 2003).

Phase III. Many of the flow sets belonging to the channelized flow of phase III do not have a spatial overlap making it difficult to evaluate their temporal relation. Nevertheless, they have been divided into temporal substages (Fig. 7C) based on the criteria listed in Ch. 5. Those flow sets that do have overlapping features show a distinct development of being increasingly dependent on underlying topography as they become more and more constrained in low-lying areas and the deeper parts of the valleys. They also show an increasing diversion from a SE directed flow, probably draining a remaining ice dome in Jotunheimen. These changes are most likely due to the vertical thinning of ice. Some of the flow directions of phase III, as well as phase II, are confirmed by the observed trend of bedrock striations (Fig. 2). Phase III with channelized ice flow with its substages can also be correlated to the *later inland phase* by Bergersen and Garnes (1972) as well to Vorren's (1977) Phase 4 of Preboreal (Early Holocene) age. Vorren (1977) states that transition from his Phase 3 to Phase 4 was gradual, although with some definite halts (sub-phases), representing periods of stagnation and/or readvance during deglaciation. This corresponds well with our observations of the transitional evolution of our phase III and its substages.

The flow sets of pre-early and early phase III were probably active for only a relatively short time as they are characterized by relatively small streamlined landforms (Fowler et al., 2013) and are overlain by younger flow sets. The pre-early phase III flow sets show ice flowing from mountain passes in the N continuing on the flatter plateau with slight diverging directions. Most likely, these flow sets represent local changes in ice dynamics. Several of the early phase III flow sets indicate ice flowing from upland areas following the local topography downward to the larger valley systems. Such local changes characteristic for both pre-early and early phase III corresponds well to the flow mode of the Nunatak phase by Garnes and Bergersen (1980). During this phase the ice surface is estimated to be at ca. 1500 m a.s.l. (Garnes and Bergersen, 1980), indicating a ca. 300 m thick ice flowing over the topographic highs within the study area. At some locations (e.g. Reinsåsen, Fig. 4C), the flow have partly modified the type A ribbed moraine from late phase II by depositing streamlined landforms on top. This suggest an increase ice velocity from late phase II to early phase III (c.f. Hättestrand and Kleman, 1999). The preservation of these early phase III flow sets where no traces of re-shaping are present indicates cold-based or at least less active ice existed in these areas afterwards, while the lower parts of the terrain served to accelerate ice flow and promote frictional heating beneath the ice (Hall and Glasser, 2003).

Similar to early phase III, the unambiguous features of middle phase III are only preserved in areas without younger ice flow. These are found along the valley sides at elevations higher than the late substage flow sets and in higher elevated SE-trending valleys. Some flow sets indicate that the ice at this time was thick enough to flow up-hill where the difference in altitude is ca. 90 m. In the late substage, ice must have been thinner as it was flowing around obstacles, following the underlying topography. Ice flow in the larger valleys occurred both during the middle and late substages (likely started already during the early substage), providing long enough time for formation of the large glacial bedforms found on the valley floors. In the Fjelldokka – Dokka valley and the Etne – Synnfjell area, the ice flow sets of middle and late substages reveal cross-cutting flow in the middle part and similar flow direction in the lower part of the valleys, supporting the idea of an inward migrating onset of ice flow. We correlate our middle and late substages with the Krusgrav deglacial phase by Garnes and Bergersen (1980) with flow following the Fjelldokka – Dokka valley system.

At this phase, ice surfaces was ca. 1100 m a.s.l. (Garnes and Bergersen, 1980), indicating a ca. 200 m thick ice for the up-hill flow of middle substage.

The largest belts of ribbed moraine (type B) are located in the upstream part of the phase III flow sets, while the downstream parts are dominated by streamlined landforms (Fig. 7). Variations of thermal conditions within the same flow set may be the reason for this uneven distribution, possibly reflecting different periods from onset to ceasing of an active flow. The type B ribbed moraines are at several places overlain by small streamlined landforms, often displaying same flow direction. This suggests close temporal relations between the landforms, as well as a transition from sluggish to fast-flow conditions (Hättestrand and Kleman, 1999). As mentioned above, the higher elevated areas surrounding these flow sets where likely covered by cold-based or less active ice, with no significant deposition of subglacial bedforms. Probably the higher peaks were ice-free as the ice surface lowered (c.f. Garnes and Bergersen, 1980).

Esker systems parallel to ice flow (III(a) in Fig. 2 and Fig. 8B, supplement no. 2 and 3) are mainly found on the valley sides and close to the onset zones of phase III flow. This indicates that they acted as conduits feeding subglacial meltwater into the valleys where ice flow occurred, affecting the ice flow dynamics. Such spatial relations are in an accordance with the inwards migrating thermal boundary described by Hättestrand and Kleman (1999). They also point to close association to the deglaciation, althougth it cannot be excluded that the eskers might have formed later. The substages of phase III, especially the late phase III substage, indicate that the ice flow was active for the last time prior to the switch to stagnant conditions and the following deglaciation by vertical down-melting of the ice (Garnes and Bergersen, 1980). The latter is identified by the abundances of lateral meltwater channels and other meltwater features as transverse eskers (Fig. 2), interpreted as indicative of crevassed, stagnant ice from the last stages of deglaciation. Such meltwater features are occasionally found in close spatial relations to ribbed moraines of the phase III flow pattern. The distribution pattern of meltwater channels confirms the down-wasting mode of the deglaciation, as described by Garnes and Bergersen (1980) and Sollid and Sørbel (1994). Garnes and Bergersen (1980) suggeste a deglaciation occurred around 9000 ^{14}C years ago (ca. 10 ka) in the neighboring valleys Espedalen and Vestre Gausdal, and similar ages can be expected for Gausdal Vestfjell area.

General development. The abundance of soft-sediment bedforms, point to widespread warm-based conditions for at least at some stages during the last glacial period. This do not exclude periods with cold-based ice as warm-based conditions may have large landscape imprint (cf. Landvik et al., 2014). The observed spatial relations between the glacial landforms in our study area support the suggestion that streamlined landforms and ribbed moraine represent a continuum of landform formation process along the ice-bed interface (e.g. Aario, 1977; Rose, 1987; Everest et al., 2005; Stokes et al., 2013; Ely et al., 2016), and thus a bedform system (Stokes and Clark, 1999, 2001; Clark and Stokes, 2003).

Development of the ice flow phases and their associated landforms, suggests a gradual lowering of the ice surface with increased topographical control. Transition from phases II to III was gradual, as seen by the configuration of flows and the difference between types of ribbed moraine characteristics for phase II and phase III (discussed below). This suggests that the regional ice flow became slower (Hättestrand and Kleman, 1999) and then reorganized into faster, active flow in the valleys during phase III (Fig. 7C), probably an effect of the transition to channelized flow. This topographically constrained ice-flow of phase III corresponds well with the concept of a 'local flow style' as described by Landvik et al. (2014). At the same time, higher elevated areas became increasing less active, probably with cold ice preserving older flow set, and eventually ice free (Garnes and Bergersen, 1980). Close spatial distribution of meltwater features with phase III landforms suggest a gradual transition to the deglacation.

7.2. Ribbed moraines - implications on glacial dynamics

The ribbed moraines identified in this study are assigned to type A (broad fields) ribbed moraines from regional flow phase II and to type B (belts) ribbed moraines from the channelized flow phase III. The reason for this division is probably only related to the topography and the vertical thinning of ice. Type A ribbed moraines are typically only found on plateaus yielding enough space for a wide distribution of moraine ridges and limiting the active ice flow to phase III. Whereas, type B are scattered throughout the whole study area, although commonly found in topographic lows, i.e. in areas with less space and active phase III ice flow. It cannot be excluded that some of the type B ribbed moraines may have initiated during phase II or at the transition to phase III. The varying locations of the ribbed moraines, from high plateaus to low-lying valleys, connect these to different phases and substages (Fig. 7). Thus, suggest that the formation of ribbed moraines occurred at different times, probably at the transition from phase II to III and at the late substage of phase III.

The formation of ribbed moraines are widely discussed, and numerous theories exist. Important factors proposed for the formation includes substrate characteristics, subglacial hydrology, ice velocity and flow conditions, and transition from cold- to warm-based conditions (Trommelen et al., 2014, and references therein). Dunlop and Clark (2006b) propose a single unifying theory should be sought to explain their genesis, whereas others (e.g. Kurimo, 1980; Finleyson and Bradwell, 2008; Möller, 2005; Möller and Dowling, 2015; Möller et al., 2016) suggest that ribbed moraine as geomorphic term should be seen as a polygenetic landform group. Though the formation mechanisms of ribbed moraine is uncertain, it is commonly agreed that they are formed subglacially under slow and sluggish ice-flow conditions (e.g.

Aario, 1977; Dunlop et al., 2008; Hättestrand, 1997; Hättestrand and Kleman, 1999; Lindén et al., 2008; Möller, 2005; Sollid and Sørbel, 1994; Sarala, 2006; Stokes et al., 2008; Trommelen et al., 2014).

Within the framework of this paper, the question is whether the occurrence of ribbed moraine represent an ice-flow stage of acceleration or deceleration in ice. Hättestrand and Kleman (1999) suggested that as cold-to warm-based conditions migrated inwards, ribbed moraine formed during ice-flow acceleration. Observations in line with this are (a) distinctly elongated streamlined landforms accompanying the ribbed moraine ridges in the down-flow direction (Fig. 2B), (b) streamlined landforms on top of ribbed moraine ridges (Figs. 2, 3C and 8) and (c) rotation of ridge-crest to subparallel alignment to the latest flow direction (Figs. 4C and 8C). Such relations are commonly found in our study area, more often within ribbed moraine belts (type B) in the low-lying valleys sloping in same direction as the ice flow. This morphological setting may have contributed to the increase flow velocity (Dunlop et al., 2008).

Observations supporting a decelerating ice flow are (a) re-worked streamlined landforms into ribbed moraines (Figs. 2D close-up and 8A) and (b) ribbed moraine ridges on top of streamlined landforms (Figs. 2D close-up and 3C) ice flow (Dunlop et al., 2008). These observations are all found within phase II flow, including the streamlined terrain and ribbed moraines in the Reinsåsen area (Figs. 2D close-up, 3C and 7C). Here, the ribbed moraine ridges lie on top of streamlined landforms or are reworked from original streamlined landforms. Deposited on top of these two bedforms are small-scale streamlined landforms belonging to phase III. From this spatial pattern at Reinsåsen, it is evident that the ribbed moraine ridges could have formed close to or during the final stage of phase II. At this time the regional ice flow must have gradually slowed down, possibly due to the stiffening of the bed, either through meltwater drainage or change in thermal regime (c.f. Stokes et al., 2013).

In the Trollåsen area (Figs. 2C, 5), ice was flowing uphill in the narrow, confined valley, crossing over a pass into the lower-lying Etne valley during phase II. Similar constrained and uphill flow of ice is observed in other parts of the study area (e.g. in W of Fig. 8C). These topographical conditions are favorable for compressional (and decelerating) ice flow with shear and stack processes (e.g. Lindén et al., 2008; Stokes et al., 2008), and was probably the driving mechanism for formation of the ribbed moraine field here. Such compressional conditions must have produced excess of subglacial meltwater that likely drained through a meltwater channel, initially subglacial, from Trollåsen to Etne valley (close-up in Fig. 2C), and as elsewhere feeding the subglacial drainage system. This provided additional meltwater input to Etne valley, and such water-rich conditions must have affected the formation of ribbed moraines here. Moreover, the spatial distribution of parallel esker systems in the whole study area suggest high input of subglacial meltwater close to type B ribbed moraines. Therefore, we admit the connection between ribbed moraine formation and meltwater occurrence, and to some limited extent, agree on Sollid and Sørbel's (1994) interpretations that ribbed moraines are formed in areas with isolated patches of subglacial water bodies.

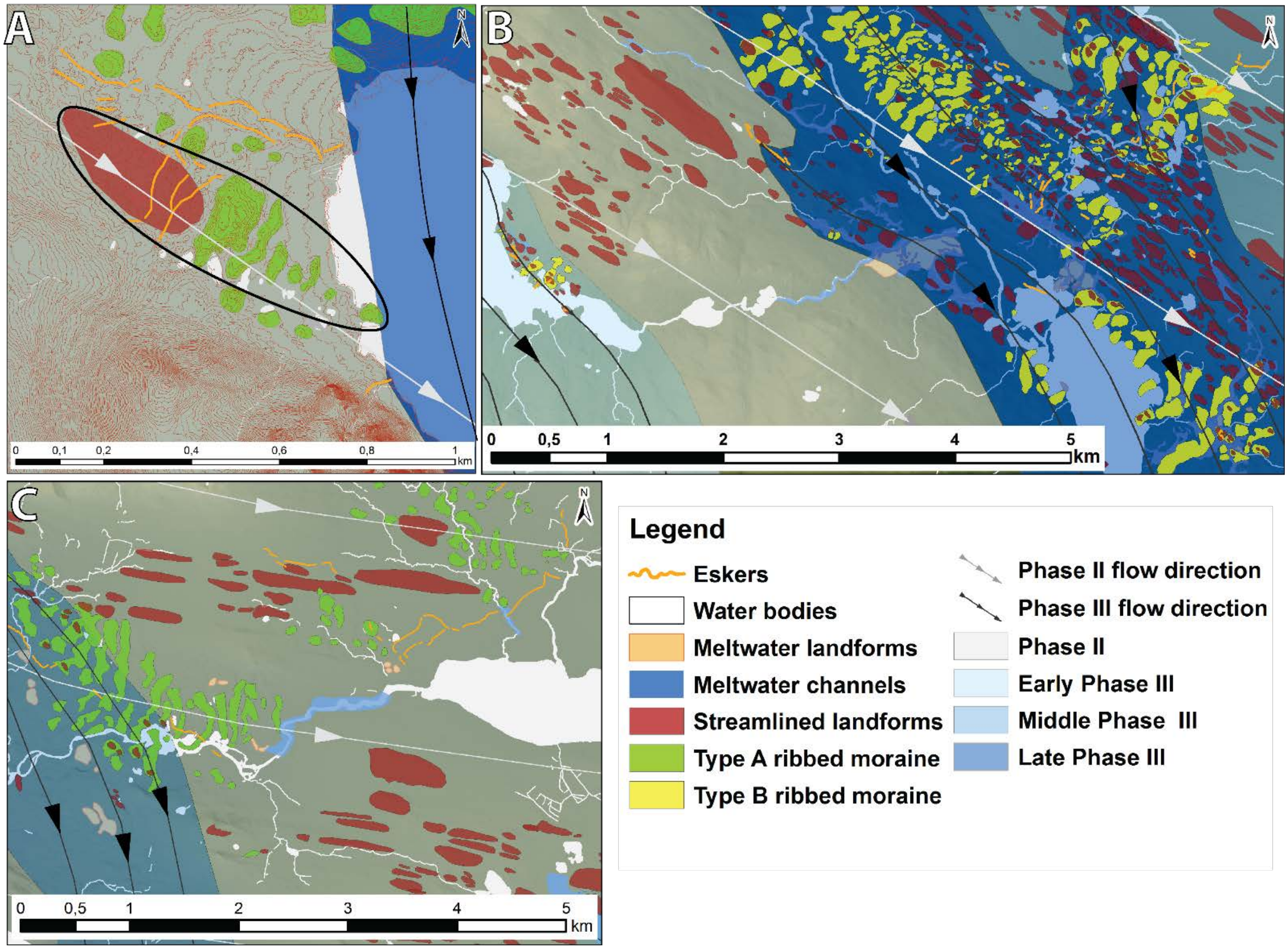

Figure 8. Glacial landforms plotted on reconstructed ice flow sets (details from Fig. 7), showing examples of ribbed moraine formation in connection to the slowdown of the regional ice flow (phase II). **A.** Previous streamlined landform (outlined in black) reworked into ribbed moraines in downstream (eastern) part. Both bedforms belong to phase II. Map excerpt from the western part of study area (0.5 m contour intervals). **B.** Ribbed moraine overlain by streamlined landforms in Etne valley. Small overlying streamlined landforms are of late phase III age. **C.** Streamlined terrain and ribbed moraine fields of phase II located close to Lake Yddin. They are partly affected by the younger phase III flow as seen by overlying small streamlined landforms and re-orientation of some ribbed moraine ridges.

8. Conclusions

The extensive mapping of spatial distribution pattern of glacial landforms carried out during this study, has revealed new insight on the development of ice flow pattern and ice flow dynamics during the Late Weichselian within the inner areas of the Fennoscandian Ice Sheet.

- The reconstructed flow pattern reveals a stepwise evolution where the *topographically independent flow (phase I)* with the maximum ice sheet thickness succeeded by the *regional flow (phase II).*
- Following a gradual transition is the *channelized flow (phase III)* with several substages, prior to the complete deglaciation by a vertical wastage meltdown. The flow sets in phase III reflect gradually stronger dependence on topography. Cold-based or less active ice conditions prevailed between the flow sets.
- Esker systems parallel to ice flow likely fed the subglacial drainage network within the valleys during phase III, while transverse esker systems probably formed in crevasses of dead ice during the late stages of deglaciation.
- All of the identified flow phases show unambiguous ice flow towards the SE, thus the ice divide must have been to the NW. This suggests that close to the study area, the ice divide was located at a more westerly position, at least as far W and N as possible within the late ice divide zone by Vorren (1977).
- Ribbed moraine formation can occur both when the ice flow slows down (identified by various re-worked streamlined landforms and ribbed moraine ridges on top of streamlined landforms) and speeds up (ribbed moraine ridges overlaid by streamlined landforms, both belonging to phase III). This implies that the 'ribbed moraine' should be regarded as a geomorphic term used for a polygenetic landform group (identifying transverse-to-ice-flow ridges), and the landforms of this group are a subject to the principles of equifinality. Further, ribbed moraine formation seems to have occurred prior to the latest stages of phase II (by deceleration) and of phase III (by acceleration).

Acknowledgements

The authors would like to thank Jon Landvik for valuable input and discussion, Leif Vidar Jakobsen, Håvard Tveite and Sverre Anmarkrud for the technical support, the Norwegian Mapping Authority (Kartverket) for providing the LiDAR data set and Renata Lapinska-Viola (NGU) for helping on acquiring additional data sets of the study area. Thanks to the reviewers for constructively comments. The fieldwork was funded by NMBU-project TverrForsk.

References:

Aario, R., 1977. Classification and terminology of morainic landforms in Finland. Boreas 6, 87-100.

Bergersen, O.F., Garnes, K., 1971. Evidence of sub-till sediments from a Weichselian interstadial in the Gudbransdalen valley, entral East Norway. Norsk Geologisk Tidsskrift 25, 99-108.

Bergersen, O.F., Garnes, K., 1972. Ice movements and till stratigraphy in the Gudbransdal area. Preliminary results. Norsk Geologisk Tidsskrift 26, 1-16.

Bergersen, O.F., Garnes, K., 1981. Weichselian in Central South-Norway - The Gudbrandsdal Interstadial and the following glaciation. Boreas 10, 315-322.

Böse, M., Luthgens, C., Lee, J.R., Rose, J., 2012. Quaternary glaciations of northern Europe. Quaternary Science Reviews 44, 1-25.

Boulton, G., Hagdorn, M., 2006. Glaciology of the British Isles Ice Sheet during the last glacial cycle: form, flow, streams and lobes. Quaternary Science Reviews 25, 3359-3390.

Briner, J.P., 2007. Supporting evidence from the New York drumlin field that elongate subglacial bedforms indicate fast ice flow. Boreas 36, 143-147.

Carlson, A.B., Sollid, J.L., 1979. *Fullsenn, kvartærgeologisk kart 1717 III - 1:50 000*. Norges geologiske undersøkelse, Trondheim.

Carlson, A.B., Sollid, J.L., 1983. Fullsenn. Beskrivelse til kvartærgeologisk kart 1717 III – M 1:50 000 *Norges geologiske undersøkelse* 390. 1-35 NGU, Trondheim.

Clark, C.D., 1993. Mega-scale glacial lineations and cross-cutting ice-flow landforms. Earth Surface Processes and Landforms 18, 1-29.

Clark, C.D., 1997. Reconstructing the evolutionary dynamics of former ice sheets using multi-temporal evidence, remote sensing and GIS. Quaternary Science Reviews 16, 1067-1092.

Clark, C.D., Hughes, A.L.C., Greenwood, S.L., Jordan, C., Sejrup, H.P., 2012. Pattern and timing of retreat of the last British-Irish Ice Sheet. Quaternary Science Reviews 44, 112-146.

Clark, C.D., Stokes. C.R., 2003. Palaeo-ice stream landsystem. In: Evans, D.J.A. (Ed.), Glacial Landsystems. London, Hodder Arnold.

Dahl, S.O., Linge, H., Fabel, D., Murray, A.S., 2010. Extent and timing of the Scandinavian Ice Sheet during Late Weichselian (MIS3/2) glacier maximum in central southern Norway—link to the Norwegian Channel Ice Stream? Abstr. Proc. Geol. Soc. Norway 1–2010, 37–38.

Damsgaard, A., Egholm, D.L., Piotrowski, J.A., Tulaczyk, S., Larsen, N.K., Brædstrup, C.F., 2015. A new methodology to simulate subglacial deformation of water-saturated granular material. The Cryosphere 9, 2183-2200.

Dunlop, P., Clark, C.D., 2006a. Distribution of ribbed moraine in the Lac Naococane region, Central Québec, Canada. Journal of Maps 2, 59-70.

Dunlop, P., Clark, C.D., 2006b. The morphological characteristics of ribbed moraine. Quaternary Science Reviews 25, 1668-1691.

Dunlop, P., Clark, C.D., Hindmarsh, R.C.A., 2008. Bed ribbing instability explanation: Testing a numerical model of ribbed moraine formation arising from coupled flow of ice and subglacial sediment. Journal of Geophysical Research, Earth Surface 113.

Ely, J.C., Clark, C.D., Spagnolo, M., Stokes, C.R., Greenwood, S.L., Hughes, A.L.C., Dunlop, P., Hess, D., 2016. Do subglacial bedforms comprise a size and shape continuum? Geomorphology 257, 108-119.

Evans, D.J.A., Phillips, E.R., Hiemstra, J.F., Auton, C.A., 2006. Subglacial till: Formation, sedimentary characteristics and classifications. Earth-Science Reviews 78, 115-176

Everest, J., Bradwell, T., Golledge, N., 2005. Subglacial landforms of the Tweed palaeo-ice stream. Scottish Geographical Journal 121, 163-173.

Eyles, N., Eyles, C.H., Miall, A.D., 1983. Lithofacies types and vertical profile models - an alternative approach to the description and environmental interpretation of glacial diamict and diamictite sequences. Sedimentology 30, 393-410.

Finlayson, A.G., Bradwell, T., 2008. Morphological characteristics, formation and glaciological significance of Rogen moraine in northern Scotland. Geomorphology 101, 607-617.

Fowler A.C., Spagnolo M., Clark C.D., Stokes C.R., Hughes A.L.C., Dunlop P. On the size and shape of drumlins. Int J Geomath. 2013; 4: 155–165. doi: 10.1007/s13137-013-0050-0

Fredin, O., Bergstrøm, B., Eilertsen, R., Hansen, L., Longva, O., Nesje, A., Sveian, H. (2013) Glacial landforms and Quaternary landscape development in Norway. In: Olsen, L., Fredin, O., Olesen, O. (Eds.), Quaternary Geology of Norway, Geological Survey of Norway Special Publication, 13, pp. 5–25.

Garnes, K., Bergersen, O.F., 1977. Distribution and genesis of tills in central South Norway. Boreas 6, 135-147.

Garnes, K., Bergersen, O.F., 1980. Wastage features of the inland ice sheet in central South Norway. Boreas 9, 251-269.

Goehring, B.M., Brook, E.J., Linge, H., Ralsbeck, G.M., Yiou, F., 2008. Beryllium-10 exposure ages of erratic boulders in southern Norway and implications for the history of the Fennoscandian Ice Sheet. Quaternary Science Reviews 27, 320-336.

Greenwood, S.L., Clark, C.D., 2009a. Reconstructing the last Irish Ice Sheet 1: changing flow geometries and ice flow dynamics deciphered from the glacial landform record. Quaternary Science Reviews 28, 3085-3100.

Greenwood, S.L., Clark, C.D., 2009b. Reconstructing the last Irish Ice Sheet 2: a geomorphologically-driven model of ice sheet growth, retreat and dynamics. Quaternary Science Reviews 28, 3101-3123.

Greenwood, S.L., Clark, C.D., Hughes, A.L.C., 2007. Formalising an inversion methodology for reconstructing ice-sheet retreat patterns from meltwater channels: application to the British Ice Sheet. J. Quat. Sci. 22, 637-645.

Hall, A.M., Glasser, N.F., 2003. Reconstructing the basal thermal regime of an ice stream in a landscape of selective linear erosion: Glen Avon, Cairngorm Mountains, Scotland. Boreas 32, 191-207.

Hättestrand, C., 1997. Ribbed moraines in Sweden - distribution pattern and palaeoglaciological implications. Sedimentary Geology 111, 41-56.

Hättestrand, C., Kleman, J., 1999. Ribbed moraine formation. Quaternary Science Reviews 18, 43-61.

Heim, M., Schärer, U., LMilnes, G., 1977. The nappe complex in the Tyin-Bygdin-Vang region, central southern Norway. *Norsk Geologisk Tidsskrift* 57, 171-181. Oslo.

Hubbard, A., Bradwell, T., Golledge, N., Hall, A., Patton, H., Sugden, D., Cooper, R., Stoker, M., 2009. Dynamic cycles, ice streams and their impact on the extent, chronology and deglaciation of the British-Irish ice sheet. Quaternary Science Reviews 28, 758-776.

Hughes, A.L.C., Clark, C.D., Jordan, C.J., 2014. Flow-pattern evolution of the last British Ice Sheet. Quaternary Science Reviews 89, 148-168.

Hughes, A.L.C., Gyllencreutz, R., Lohne, Ø.S., Mangerud, J., Svendsen, J.I., 2016. The last Eurasian ice sheets – a chronological database and time-slice reconstruction, DATED-1. Boreas 45, 1-45.

Kleman, J., Glasser, N.F., 2007. The subglacial thermal organisation (STO) of ice sheets. Quaternary Science Reviews 26, 585-597.

Kleman, J., Hättestrand, C., Borgstrom, I., Stroeven, A., 1997. Fennoscandian palaeoglaciology reconstructed using a glacial geological inversion model. J. Glaciol. 43, 283-299.

Knight, J., 2010. Basin-scale patterns of subglacial sediment mobility: Implications for glaciological inversion modelling. Sedimentary Geology 232, 145-160.

Knight, J., 2011. Subglacial processes and drumlin formation in a confined bedrock valley, northwest Ireland. Boreas 40, 289-302.

Kurimo, H., 1980. Depositional deglaciation forms as indicators of different glacial and glaciomarginal environments. Boreas 9, 179-191.

Landvik, J.Y., Alexanderson, H., Henriksen, M., Ingólfsson, Ó., 2014. Landscape imprints of changing glacial regimes during ice-sheet build-up and decay: a conceptual model from Svalbard. Quaternary Science Reviews 92, 258-268.

Larsen, N.K., Piotrowski, J.A., 2003. Fabric pattern in a basal till succession and its significance for reconstructing subglacial processes. J. Sediment. Res. 73, 725-734.

Le Heron, D.P., Etienne, J.L., 2005. A complex subglacial clastic dyke swarm, Sólheimajökull, southern Iceland. Sedimentary Geology 181, 25-37.

Lindén, M., Möller, P. & Adrielsson, L., 2008. Ribbed moraine formed by subglacial folding, thrust stacking and lee-side cavity infill. *Boreas 37/1*, 102–131.

Mangerud, J., 2004. Ice sheet limits on Norway and the Norwegian continental shelf, Developments in Quaternary Science. Elsevier, pp. 271-294.

Mangerud, J., Gyllencreutz, R., Lohne, Ø., Svendsen, J.I., 2011. Glacial History of Norway. In: Ehlers, J., Gibbard, P.L., Hughes, P.D. (Eds.), Developments in Quaternary Sciences. Elsevier, pp. 279-298.

Mangerud, J., Larsen, E., Longva, O., Sønstegaard, E., 1979. Glacial history of western Norway 15,000-10,000 BP. Boreas 8, 179-187.

Möller, P., 2005. Rogen moraine: an example of glacial reshaping of pre-existing landforms. Quaternary Science Reviews 25, 362-389.

Möller, P., 2010. Melt-out till and ribbed moraine formation, a case study from south Sweden. S*edimentary Geology 232*, 161-180.

Möller, P., Dowling, T.P.F., 2015. The importance of thermal boundary transitions on glacial geomorphology; mapping of ribbed/hummocky moraine and streamlined terrain from LiDAR, over Småland, South Sweden. *GFF 137 (4),* 452-283.

Möller, P., Dowling, T.P.F., Cleland, C., Johnson, M.D., 2016: On the issue of equifinality in glacial geomorphology. Geophysical Research abstracts vol 18, EGU2016-13626. EGU General Assembly 2016.

Nesje, A., 1992. Geometry, thickness and isostatic loading of the Late Weichselian Scandinavian ice sheet. Norsk geologisk tidsskrift 72, 271-273.

Nesje, A., Dahl, S.O., Anda, E., Rye, N., 1988. Block fields in Southern-Norway - significance for the Late Weichselian Ice-Sheet. Norsk Geologisk Tidsskrift 68, 149-169.

Nickelsen, R.P., 1988. *Fullsenn 1717 III, berggrunnskart* M *1:50 000*. Norges geologiske undersøkelse.

Olsen, L., 1985. Weichselian till stratigraphy in the Lillehammer area, southeast Norway. Norsk Geologisk Undersøkelse 401, 59-81.

Olsen, L., Sveian, H., Bergstrøm, B., Ottesen, D. and Rise, L. (2013) Quaternary glaciations and their variations in Norway and on the Norwegian continental shelf. In Olsen, L.,Fredin, O. and Olesen, O. (eds.) Quaternary Geology of Norway, Geological Survey of Norway Special Publication, 13, pp. 27–78.

Ottesen, D., Dowdeswell, J.A., Rise, L., 2005. Submarine landforms and the reconstruction of fast-flowing ice streams within a large Quaternary ice sheet: The 2500-km-long Norwegian-Svalbard margin (57°–80°N). Geological Society of America Bulletin 117, 1033-1050.

Roberts, D.H., Long, A.J., 2005. Streamlined bedrock terrain and fast ice flow, Jakobshavns Isbrae, West Greenland: implications for ice stream and ice sheet dynamics. Boreas 34, 25-42.

Rose, J. 1987. Drumlins as part of a glacier bedform continuum. In: Menzies, J., Rose, J. (Eds), Drumlin Symposium. Rotterdam, Balkema, 103-116.

Ross, M., Campbell, J.E., Parent, M., Adams, R.S., 2009. Palaeo-ice streams and the subglacial landscape mosaic of the North American mid-continental prairies. Boreas 38, 421-439.

Sarala, P., 2006. Ribbed moraine stratigraphy and formation in southern Finnish Lapland. J. Quat. Sci. 21, 387e398

Sejrup, H.H., Nygård, A., Hall, A.M, Haflidason, H., 2009. Middle and Late Weichselian (Devensian) glaciation history of south-western Norway, North Sea and eastern UK. Quaternary Science Reviews 28, 370-380.

Siedlecka, A., Nystuen, J.P., Englund, J.O., Hossack, J., 1987. Lillehammer- berggrunnskart M. 1:250 000. Norges geologiske undersøkelse, Trondheim.

Sollid, J.L., Sørbel, L., 1994. Distribution of glacial landforms in southern Norway in relation to the thermal regime of the last continental ice sheet. Geografiska Annaler. Series A, Physical Geography 76, 25-35.

Spagnolo, M., Clark, C.D., Ely, J.C., Stokes, C.R., Anderson, J.B., Andreassen, K., Graham, A.G.C., King, E.C., 2014. Size, shape and spatial arrangement of mega-scale glacial lineations from a large and diverse dataset. Earth Surface Processes and Landforms 39, 1432-1448.

Spagnolo, M., Clark, C.D., Hughes, A.L.C., 2012. Drumlin relief. Geomorphology 153–154, 179-191.

Stokes, C.R., Clark, C.D., 1999. Geomorphological criteria for identifying Pleistocene ice streams. Annals of Glaciology 28, 67-75.

Stokes, C.R., Clark, C.D., 2001. Palaeo-ice streams. Quaternary Science Reviews 20, 1437-1457.

Stokes, C.R., Clark, C.D., Lian, O.B., Tulaczyk, S., 2007. Ice stream sticky spots: A review of their identification and influence beneath contemporary and palaeo-ice streams. Earth-Science Reviews 81, 217-249.

Stokes, C.R., Lian, O.B., Tulaczyk, S., Clark, C.D., 2008. Superimposition of ribbed moraines on a palaeo-ice-stream bed: implications for ice stream dynamics and shutdown. Earth Surface Processes and Landforms 33, 593-609.

Stokes, C.R., Spagnolo, M., Clark, C.D., 2011. The composition and internal structure of drumlins: Complexity, commonality, and implications for a unifying theory of their formation. Earth-Science Reviews 107, 398-422.

Stokes, C.R., Spagnolo, M., Clark, C.D., Ó Cofaigh, C., Lian, O.B., Dunstone, R.B., 2013. Formation of mega-scale glacial lineations on the Dubawnt Lake Ice Stream bed: 1. size, shape and spacing from a large remote sensing dataset. Quaternary Science Reviews 77, 190-209.

Svendsen, J.I., Alexanderson, H., Astakhov, V.I., Demidov, I., Dowdeswell, J.A., Funder, S., Gataullin, V., Henriksen, M., Hjort, C., Houmark-Nielsen, M., Hubberten, H.W., Ingolfsson, O., Jakobsson, M., Kjaer, K.H., Larsen, E., Lokrantz, H., Lunkka, J.P., Lysa, A., Mangerud, J., Matiouchkov, A., Murray, A., Moller, P., Niessen, F., Nikolskaya, O., Polyak, L., Saarnisto, M., Siegert, C., Siegert, M.J., Spielhagen, R.F., Stein, R., 2004. Late quaternary ice sheet history of northern Eurasia. Quaternary Science Reviews 23, 1229-1271.

Svendsen, J.I., Briner, J.P., Mangerud, J., Young, N.E., 2015. Early break-up of the Norwegian Channel Ice Stream during the Last Glacial Maximum. Quaternary Science Reviews 107, 231-242.

Trommelen, M., Ross, M., 2010. Subglacial landforms in northern Manitoba, Canada, based on remote sensing data. Journal of Maps 6, 618-638.

Trommelen, M.S., Ross, M., Ismail, A., 2014. Ribbed moraines in northern Manitoba, Canada: characteristics and preservation as part of a subglacial bed mosaic near the core regions of ice sheets. Quaternary Science Reviews 87, 135-155.

van der Meer, J.J.M., Kjær, K.H., Krüger, J., Rabassa, J., Kilfeather, A.A., 2009. Under pressure: clastic dykes in glacial settings. Quaternary Science Reviews 28, 708-720.

Vorren, T.O., 1977. Weichselian Ice Movement in South-Norway and adjacent areas. Boreas 6, 248-257.